Hybrid meson production by electromagnetic and weak interactions in a flux-tube model

F. E. Close* and J. J. Dudek†
Department of Physics—Theoretical Physics, University of Oxford, 1 Keble Rd., Oxford OX1 3NP, United Kingdom
(Received 28 October 2003; published 26 February 2004)

We calculate rates for hybrid meson production by electromagnetic and weak interactions in the flux-tube model. Applications include photoproduction and electroproduction at Jefferson Laboratory and DESY HERA, and the production of light strange and charmed hybrids in the weak decays of heavy flavors. Photoproduction of some light hybrids is predicted to be prominent in charge exchange reactions, $\gamma p \to n\mathcal{H}$ and accessible in $\gamma p \to p\mathcal{H}$. Production of light or charmed hybrids in B and D decays may be feasible with high statistics. Photoproduction of the axial hybrid meson is predicted to be large courtesy of π exchange, and its strange counterpart is predicted in $B \to \psi K_H(1^+)$ with BR$\sim 10^{-4}$. Production rates for exotic hybrid candidates $1^{-+};(0,2)^{+-}$ are given special attention. Selection rules that can help to distinguish between hybrid and conventional states with the same J^{PC} are noted.

DOI: 10.1103/PhysRevD.69.034010 PACS number(s): 12.39.Mk, 12.38.Lg, 13.60.Le

I. INTRODUCTION

An outstanding problem in the standard model is how the non-Abelian, gluon, degrees of freedom behave in the limit of strong QCD. Lattice QCD predicts a spectroscopy of glueballs [1] and hybrid mesons [2], but there are no unambiguous signals against which these predictions can be tested.

A major stumbling block in the case of hybrids is that while predictions for their masses [2,3], hadronic widths [4,5], and decay channels [4–6] are rather well agreed upon, the literature contains no general discussion of their production rates in electromagnetic or weak interactions. Meanwhile a significant plank in the proposed upgrade of Jefferson Laboratory is its assumed ability to expose the predicted hybrid mesons in photoproduction and electroproduction.

Theory [3,7] has provided compelling arguments from QCD that confinement occurs via the formation of a flux tube. In the simplest situation of a long tube with fixed $Q,\overline{Q}$ sources on its ends, a flux tube has a simple vibrational spectrum corresponding to the excitation of transverse phonons in its stringlike structure. There is a question whether the flux tube is fully formed on the $O(1)$ fm scale typical of hadrons [Ref. [8] suggests that at $O(1)$ fm the state of confined gluon fields is between that typical of bag models and those of a fully formed flux tube; by contrast [9] finds that the flux tube forms at distances below 1 fm]. The model of Ref. [3] assumes that the fully formed tube drives the phenomenology and that the essential features of this gluonic spectrum are retained in the spectrum of real mesons with their flux-tube excited: the hybrid mesons.

The flux-tube model has not been derived from QCD, but it is currently the best that we have that builds on features emerging from the strong coupling limit of QCD. Hopefully its successes or failings can enable deeper insights to emerge as to the dynamics of QCD in the strong interaction limit. It leads to the effective linear potential of the conventional meson spectroscopy and has an identical $N=1$ spectrum of hybrid states as the lattice—a feature that is especially relevant to the present calculations. As well as reproducing the results of lattice QCD, such as the spectroscopy of conventional and hybrid states, it can also stimulate deeper studies by investigating areas where lattice methods have not yet been applied. For example, the flux-tube model predicted that decays of hybrids to ground state mesons are suppressed relative to those to excited states [3,5], which has recently been confirmed within the lattice framework [10]. We would hope that insights from the present work in their turn might inspire future lattice studies, which could thereby better establish their connection with reality.

While the flux-tube model has limitations, it may be the best way forward at present for developing insights into production dynamics and related phenomenology. In such a context, it is playing a prominent role in the Jefferson Laboratory upgrade proposal, where it has been used to underpin much of their planning. To turn this into something of practical use will require predictions for the electromagnetic transition amplitudes to hybrid mesons. However, while implications for spectroscopy and hadronic decays in such a model have been extensively explored, previous estimates of electromagnetic couplings in this model (Refs. [11,12]) are at best only upper limits, in that they were based upon vector meson dominance of hadronic decays of hybrids into modes including ρ and further assumed that the predicted suppression of decay into $\pi\rho$ is suspended in π exchange. We are unaware of any direct calculation of photoproduction or electroproduction of hybrids in this model. This is the issue that we address in this paper.

From among the results of our extensive survey we note the following.

(1) The electric dipole transitions of the hybrid axial meson to $\pi^{\pm}\gamma$ and of the exotic $(0,2)^{+-}$ to $\rho\gamma$ give radiative widths that can exceed 1 MeV. This implies significant photoproduction rates in charge exchange reactions $\gamma p \to \mathcal{H}^{+} n$. The exotic 2^{+-} may also be produced diffractively in $\gamma p \to \mathcal{H} p$.

(2) ''Wrong G-parity'' electric dipole matrix elements provide a measure of the penalty for exciting gluonic degrees

*Email address: f.close@physics.ox.ac.uk
†Email address: dudek@thphys.ox.ac.uk

 ©2004 The American Physical Society

of freedom. We suggest how a study within lattice QCD might generalize and underpin this by computing spin-nonflip $E1$ matrix elements from π to $J^P=1^+$ final states with G parity $=\pm 1$, or analogous transitions from ρ.

(3) The production of an axial strange hybrid in $B \to \psi K_H$ is predicted to have BR$\sim O(10^{-4})$ as long as its mass $\leqslant 2.1$ GeV. There is a tantalizing unexplained enhancement in the data that may be compatible with this [13] and merits further investigation.

(4) If there is a light exotic hybrid [14–17] with $J^{PC}=1^{-+}$, the $I=1$ and $I=0$ states could be produced in $D \to \pi\mathcal{H}$ and $D_s \to \pi\mathcal{H}$ with branching ratios $\sim 10^{-7}$, or more promisingly in $B \to D^{(*)}\mathcal{H}$ with a branching ratio comparable to $B \to D\rho$, although this second prediction is somewhat model dependent.

(5) Measurement of the axial to vector amplitude ratio in $B \to D_{(H)}X$ may enable the hybrid content of charmed mesons to be determined.

II. MODEL

The flux tube is a relativistic object with an infinite number of degrees of freedom. A standard approximation [3–5,18] has been to fix the longitudinal separation of the $Q\overline{Q} \equiv r$ and to solve the flux-tube dynamics in the limit of a thin relativistic string with purely transverse degrees of freedom. The resulting energies $E(r)$ are then used as adiabatic effective potentials on which the meson spectroscopies are built. Reference [19] studied the effect of relaxing these strict approximations and found that the spectrum of the conventional and lowest hybrids is robust. We shall assume the same is true in this first calculation of electromagnetic excitation of hybrid mesons.

In Refs. [3,18,19] the flux tube was discretized into $N+1$ cells (modern lattice computations typically have $N \sim 10$) and then $N \to \infty$. Up to N modes may be excited. We shall focus on the first excited state, with excitation energy $\omega = \pi/r$ where r is the length of the flux tube. If the length of a cell is l, then $r=(N+1)l$.

The state of the flux tube can be written in terms of a complete set of transverse eigenstates,

$$|\vec{y}\rangle = |\vec{y}_1 \cdots \vec{y}_n \cdots \vec{y}_N\rangle,$$

and the Fourier mode for the first excited state[1] is

$$\vec{a} = \sqrt{\frac{2}{N+1}} \sum_{n=0}^{N} \vec{y}_n \sin\frac{\pi n}{N+1} \tag{1}$$

or

$$\vec{y}_n = \sqrt{\frac{2}{N+1}} \vec{a} \sin\frac{\pi n}{N+1}. \tag{2}$$

[1]Higher modes (up to $p=N$) exist but we are not interested in them here as we wish to specialize to the lightest hybrid mesons. Incorporating such modes is straightforward in the formalism we describe.

The oscillations are in the two-dimensional space transverse to the nominal $Q\overline{Q}$ axis. Thus there are two Fourier modes $\vec{a} \equiv (a_1, a_2)$ where 1, 2 refer to the two (body-fixed) orthogonal coordinate directions, $\hat{e}_1, \hat{e}_2$.

In the small oscillation approximation the system becomes harmonic in $\vec{y}$ $(\vec{a})$. Then if b is the string tension ($b \sim 1$ GeV/fm), the eigenfunctions for the ground and first excited states (labeled 0 and 1, respectively) are in Fourier-mode space:

$$\chi_0(a_{1,2}) = \left(\frac{b}{N+1}\right)^{1/4} \exp\left[-\frac{b\pi}{2(N+1)} a_{1,2}^2\right], \tag{3}$$

$$\chi_1(a_{1,2}) = \sqrt{\frac{2b\pi}{N+1}} a_{1,2} \chi_0(a_{1,2}). \tag{4}$$

To reduce the number of indices write $\vec{a} \equiv (a_1, a_2)$ in the body-fixed basis and understand any $\vec{a}$ to refer always to these components. To proceed to the continuum, write (see [3,18])

$$\frac{b\pi}{N+1} \equiv \beta_1^2.$$

The Gaussian wave functions, Eqs. (3),(4), for the flux-tube ground state and first excited mode become

$$\chi_0(\vec{a}) = (\beta_1^2/\pi)^{1/4} \exp[-\beta_1^2 \vec{a}^2/2], \tag{5}$$

$$\chi_1(\vec{a}) = \sqrt{2}\beta_1 \vec{a} \chi_0(\vec{a}). \tag{6}$$

The wave functions for mesons must include the state of the flux tube; for conventional mesons, where the flux tube is in its ground state, write

$$\mathcal{C} = \psi^{(0)}_{nlm}(\vec{r}) \chi_0(a_1) \chi_0(a_2),$$

where n,l,m are the usual two-body quantum numbers and the subscript zero indicates the ground state. If either of the transverse modes is excited, one has a state that we refer to as a hybrid meson. The particular combinations $(1/\sqrt{2})[a_1 \pm i a_2] \equiv (1/\sqrt{2}) a^{\pm}$ give normalized circularly polarized phonon modes for the flux tube, which have angular momentum ± 1 about the longitudinal $(Q\overline{Q})$ axis. The corresponding wave function for such a hybrid may be summarized by

$$\mathcal{H} = \psi^{(\pm)}_{nlm}(\vec{r}) \frac{1}{\sqrt{2}} [\chi_1(a_1)\chi_0(a_2) \pm i \chi_0(a_1)\chi_1(a_2)]$$

or

$$\mathcal{H} = \psi^{(\pm)}_{nlm}(\vec{r}) \beta_1 (a_1 \pm i a_2) \chi_0(a_1) \chi_0(a_2).$$

The challenge is, how can electromagnetic or weak currents, which couple to quarks, break the orthogonality of $\langle \vec{a} \rangle$ needed to give a transition between conventional and (first) excited flux-tube (hybrid) state? The answer is implicit in the observation of Isgur [18] that the flux tube is a dynamic

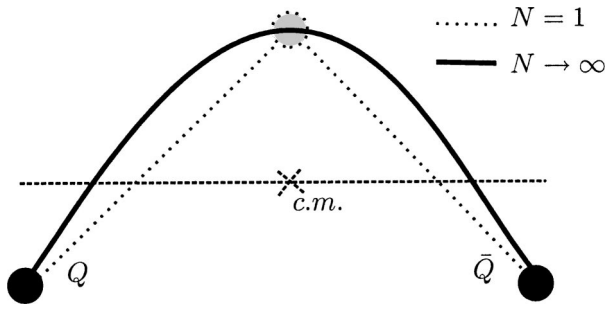

FIG. 1. $p=1$ mode hybrid structure.

entity, with a zero-point motion which can affect observables that at first sight are driven by the Q or $\bar{Q}$.

The physical picture becomes transparent if one simulates the tube as a series of beads with mass m on a massless string and simplifies to the cases of $N=1,2$ [20]. We will be interested here in excitation of the first hybrid mode, whose essential spatial structure can be simulated by a single bead of mass $m\equiv br$.

In this first excited mode the center of mass of the $Q\bar{Q}$-bead system is displaced from the interquark axis by a transverse distance that scales as $\sim m/m_Q$. If the transverse displacement of the bead is $\vec{y}$ and the Q and $\bar{Q}$ have masses m_Q, then relative to the center of mass, the position vector of the quark (antiquark) has components in the longitudinal $\vec{r}$ and transverse $\vec{y}$ directions:

$$\vec{r}_{Q(\bar{Q})}=\left[\pm\frac{1}{2}\vec{r};\left(\frac{br}{2m_Q}\right)\vec{y}\right]. \tag{7}$$

The dependence of $\vec{r}_{Q(\bar{Q})}$ on $\vec{y}$ enables a quark-current interaction to excite transitions in the $\vec{y}$ oscillator, leading to excitation of the flux tube. The presence of $\pm$ in the $\vec{r}$ coordinate, but only $+$ in the case of $\vec{y}(\vec{a})$, is a feature of the first excited mode. This is illustrated for the full flux tube in Fig. 1. The longitudinal axis passes through the c.m. of the system. If the tube's effective c.m. (the "bead") is displaced transverse to this in one direction; then, the Q and $\bar{Q}$ respond collectively to the displacement of the flux tube and are both on the opposite side of the longitudinal axis. Hence the same sign appears in the $\vec{y}(\vec{a})$ coordinate, but opposite signs in the longitudinal $\pm\vec{r}$. This sign will have significant consequences when we discuss $E1$ transitions.

This is the essential physics behind the excitation of hybrid modes by current interactions with the quark or antiquark.

Extending to N beads [18] leads to more mathematical detail and enables excitations of up to N modes, but the underlying principles are the same. The position vector becomes

$$\vec{r}_{Q(\bar{Q})}=\vec{R}\pm\frac{1}{2}\vec{r}-\vec{a}\frac{br}{\pi m_Q}\sqrt{\frac{2}{N+1}} \tag{8}$$

or, in the continuum limit,

$$\vec{r}_{Q(\bar{Q})}=\vec{R}\pm\frac{\vec{r}}{2}-\vec{a}\frac{r}{m_Q}\beta_1\sqrt{\frac{2b}{\pi^3}}. \tag{9}$$

The essential physics is already contained in the above examples. For modes with $p=$ even, the moment of the tube deformation relative to the interquark axis tends to cancel, leading to a null displacement of the quarks. For $p=$ odd, the tube has a net transverse moment, leading to a compensating transverse displacement of the quark(s). This is encoded in the factor $(-1)^p$ for the quark displacement in the pth mode in Isgur's formulation [Eq. (16) of [18]].

Isgur [18] noted that the dynamical degree of freedom implicit in the $\vec{y}$ (or $\vec{a}$) gives a hitherto overlooked (but welcome) contribution to the charge radius in elastic form factors. This comes about because the Coulomb interaction with the quark $F_{\rm el}(\vec{q})=\langle{\rm g.s.}|e^{i\vec{q}\cdot\vec{r}_Q}|{\rm g.s.}\rangle$ receives contributions from both the $\vec{r}$ and $\vec{a}$ degrees of freedom at $\mathcal{O}(q^2r^2)$ and $\mathcal{O}(q^2a^2)$.

In the continuum limit $N\to\infty$ this becomes [compare Eqs. (29) *et seq* in Isgur]

$$F_{\rm el}(\vec{q})=1-\frac{|\vec{q}|^2\langle r^2\rangle}{24}\left(1+\frac{8b}{m_Q^2\pi^3}\sum_p\ \frac{1}{p^3}\right), \tag{10}$$

where the sum is over the $p=1,\ldots,\infty$ "phonon" modes (elsewhere in most of this paper we consider only the $p=1$ mode). It was shown [18] that these "transverse excursions" give large $\sim 51\%$ corrections in light quark systems where $m_Q=m_d$, and $\sim 13\%$ corrections in heavy-light $Q\bar{q}$ systems. Furthermore, the $\Sigma_1^\infty(1/p^3)$ is $\sim 80\%$ saturated by its $p=1$ term. Together, these suggested that the transition amplitudes to the lowest hybrids ($p=1$ phonon modes) could be substantial.

This is our point of departure. Expanding the incoming plane wave to leading order in the momentum transfer,

$$\exp\left[-i\vec{q}\cdot\left(\frac{1}{2}\vec{r}-\vec{a}\frac{r}{m_Q}\beta_1\sqrt{\frac{2b}{\pi^3}}\right)\right]$$
$$\to\left(1-i\frac{1}{2}\vec{q}\cdot\vec{r}\right)\left(1+i\vec{q}\cdot\vec{a}\frac{r}{m_Q}\beta_1\sqrt{\frac{2b}{\pi^3}}\right), \tag{11}$$

the linear terms in $\vec{r}$ and $\vec{a}$ break the orthogonality of initial and final wave functions and cause transitions: $E1$ excitation to $L=1$ conventional states in the case of $\vec{r}$ and excitation of the first flux-tube mode (hybrid) in the case of $\vec{a}$. By combining the above with the tensor decomposition of the current-quark interaction, we may calculate electromagnetic and weak excitation amplitudes to hybrids and compare with those for conventional mesons in various multipoles.

First we take the continuum limit, define wave functions for both hybrid and conventional states including the flux tube, illustrate the familiar $E1$ electromagnetic transition, and then calculate its analogue for hybrid excitation with specific reference to the angular integrations. The elec-

TABLE I. Naming convention for light quark hybrid mesons.

J_H^{PC}	S_{qq}	$I=1$	$I=0$
1^{++}	0	a_{1H}	f_{1H}
1^{--}	0	ρ_H	ω_H
$(0,1,2)^{+-}$	1	b_{JH}	h_{JH}
$(0,1,2)^{-+}$	1	π_{JH}	η_{JH}

troweak transitions of heavy flavors will then be described; this requires knowledge of the decomposition of V_μ and A_μ for heavy-light systems.

When $m_Q \neq m_{\bar{Q}}$ Isgur's decomposition of the position vectors [18] is

$$\vec{r}_{Q(d)} = \vec{R} \pm \vec{r}\frac{\mu}{m_{Q(d)}} - \vec{a}\frac{\beta_1 r}{m_{Q(d)}}\sqrt{\frac{2b}{\pi^3}}, \tag{12}$$

where $\mu \equiv m_Q m_d/(m_Q+m_d)$.

For nomenclature we shall adopt the PDG [21] notation, where the subscript J denotes the total angular momentum of the meson, and we append the subscript H to denote hybrid (thus for light flavors we have the notation in Table I, with obvious generalization for flavored states). This is done for two reasons: (i) to enable the trivial distinction between hybrid and conventional states to be immediately apparent and reduce confusion in the text and (ii) as a reminder that for a conventional and hybrid meson with the same overall J^{PC}, their internal $q\bar{q}$ spin states are inverted.

This spin inversion is also illustrated in Table I and has potentially important implications in helping to isolate hybrid contributions to the wave function of conventional states. For example, whereas a meson with $J^{PC}=1^{-+};(0,2)^{+-}$ has exotic correlations of J^{PC} inaccessible to conventional mesons, the other states could *a priori* be conventional or hybrid. Note, however, that the $1_H^{\pm\pm}$ have $S_{qq}=0$ whereas their conventional counterparts $1^{\pm\pm}$ have $S_{qq}=1$. Conversely, the $(0,2)_H^{-+}$ and 1_H^{+-} all have $S_{qq}=1$ whereas their conventional counterparts all have $S_{qq}=0$. Hence there is a complete spin inversion between conventional states and their hybrid counterparts.

This spin inversion enables a dynamical distinction to ensue between these two types of state, which is manifested in certain selection rules. This has already been noted in hadronic decays [5] and will have consequences in current transitions too. Furthermore, we will find that the hierarchy of spin operators leading to certain heavy flavor decays is inverted between conventional and hybrid states, such that observable consequence can ensue in principle.

III. $E1$ TRANSITIONS

A. Conventional $Q\bar{Q}$ transitions

To establish notation and make subsequent analysis of hybrid excitation more transparent, we first illustrate a conventional $E1$ transition in the nonrelativistic limit. Consider the $E1$ transition operator

$$\mathcal{O}_{E1} = -i|\vec{q}|\sum_{q=Q,d}\vec{\epsilon}_+\cdot(e_q\vec{r}_q),$$

whose essential structure when acting on a meson $Q\bar{d}$ is

$$\mathcal{O}_{E1} = -i|\vec{q}|\left\{\left(\frac{e_Q}{m_Q}-\frac{e_d}{m_d}\right)\mu\vec{\epsilon}_+\cdot\vec{r} - \left(\frac{e_Q}{m_Q}+\frac{e_d}{m_d}\right)\sqrt{\frac{2b}{\pi^3}}\beta_1 r\vec{\epsilon}_+\cdot\vec{a}\right\}.$$

If l,m denote the orbital angular momentum of the $Q\bar{d}$ system and its z projection (on fixed space axes), respectively, then the structure of the matrix element $\mathcal{M}$ becomes

$$\begin{aligned}\mathcal{M} &\equiv \langle l',m'|\mathcal{O}_{E1}|l,m\rangle \\ &= -i|\vec{q}|\left(\frac{e_Q}{m_Q}-\frac{e_d}{m_d}\right)\mu\int d^3\vec{r}\int d^2\vec{a} \\ &\quad\times\psi^{(0)*}_{n'l'm'}(\vec{r})\chi_0^*(a_1)\chi_0^*(a_2)\vec{\epsilon}_+\cdot\vec{r}\,\psi^{(0)}_{nlm}(\vec{r})\chi_0(a_1)\chi_0(a_2).\end{aligned}$$

The integration over $d^2\vec{a}\to 1$ and the standard integral over $d^3\vec{r}$ gives a transition from $l=0$ to $l'=1$ caused by the presence of $\vec{r}$.

Separating into radial and angular parts, $\psi_{nlm}(\vec{r}) \equiv R_n(r)Y_l^m(\Omega)$, and noting that

$$\vec{\epsilon}_+\cdot\vec{r} \equiv \sqrt{\frac{4\pi}{3}}rY_1^{+1}(\Omega),$$

$\mathcal{M}$ becomes

$$-i|\vec{q}|\mu\left(\frac{e_Q}{m_Q}-\frac{e_d}{m_d}\right)\sqrt{\frac{4\pi}{3}}{}_f\langle r\rangle_i\int d\Omega\, Y_{l'}^{m'*}Y_1^{+1}Y_l^m,$$

where ${}_f\langle r\rangle_i \equiv \int r^2\,dr\,R^*_{n'}(r)rR_n(r)$.

This general formula becomes more transparent when applied to the case $l=0, l'=1$ for which

$$\mathcal{M} = -i|\vec{q}|\mu\left(\frac{e_Q}{m_Q}-\frac{e_d}{m_d}\right){}_f\langle r\rangle_i\frac{1}{\sqrt{3}}\delta_{m',+1}.$$

We are interested in the specific case

$$\mathcal{M}(\gamma\pi\leftrightarrow b_1) = i\left(\frac{e_1-e_2}{m_n}\right){}_b\langle r\rangle_\pi|\vec{q}_b|\frac{m_n}{2\sqrt{3}}\delta_{m',+1}. \tag{13}$$

In general we can write the radiative width as

$$\Gamma(A\to B\gamma) = 4\frac{E_B}{m_A}|\vec{q}|\frac{1}{2J_A+1}\sum_{m_J^A}|\mathcal{M}(m_J^A, m_J^B = m_J^A+1)|^2, \tag{14}$$

where the sum is over all possible helicities of the initial meson, and the matrix element is understood to be for a positive helicity photon.

This corresponds to the familiar $E1$ transition formalism of atomic and nuclear physics as traditionally applied to $Q\overline{Q}$ systems.

Notice that $(e_Q/m_Q - e_d/m_d)$ ensures charge-conjugation conservation; for charge-neutral systems the $Q\overline{Q}$ charges cancel but they are vectorially on opposite sides of the c.m. (''longitudinal'' electric dipole moment). Hence a nonvanishing $E1$ amplitude occurs between neutral systems (e.g., $\chi \to \gamma\psi$).

B. Transitions to hybrids

Transitions to hybrids in the first excited state of the flux tube arise from the $\vec{a}$ component of the $Q,\overline{Q}$ position operators.

We consider the general matrix element for transitions between a conventional meson and a first excited-mode hybrid with tube oscillation polarization ± 1:

$$\mathcal{M} \equiv \langle \mathrm{hyb}; \pm, m' | \mathcal{O} | \mathrm{conv}; l, m \rangle = \int d^3\vec{r} \int d^2\vec{a}\, \mathcal{H}^* \mathcal{O} \mathcal{C},$$

where (i) $\mathcal{O}$ is the essential spatial structure of the transition operator, which in this example is

$$\mathcal{O}_{E1} = i|\vec{q}| \left(\frac{e_Q}{m_Q} + \frac{e_d}{m_d} \right) \sqrt{\frac{2b}{\pi^3}} \beta_1 r \vec{\epsilon}_+ \cdot \vec{a}, \tag{15}$$

(ii) $\mathcal{C}$ is the conventional meson wave function,

$$\mathcal{C} = \psi^{(0)}_{nlm}(\vec{r}) \chi_0(a_1) \chi_0(a_2),$$

(iii) $\mathcal{H}^*$ is the hybrid wave function (complex conjugate),

$$\mathcal{H}^* = \psi^{(\pm)*}_{nlm}(\vec{r}) \beta_1 (a_1 \mp i a_2) \chi_0^*(a_1) \chi_0^*(a_2)$$

(where the flux tube is excited into a state with polarization ± 1 along its axis).

To be specific, we consider the transition between the unexcited tube and a tube that has polarization $\pm$ along its axis (the ''body axis''), which axis in turn is oriented at some angles θ, ϕ in the laboratory (the ''fixed axes'').

Later we will consider both vector and axial currents in various multipoles. In general, to have a transition between a normal meson and a hybrid, one power of $\vec{a}$ will be needed in the transition operator. The factors multiplying $\vec{a}$ will depend on the tensor structure of the current (e.g., vector or axial, transverse or longitudinal), explicit forms being given in Appendix A. Having identified the presence of $\vec{a}$ we need to be able to compute its expectation value. This is outlined in Appendix B for a ''reference'' operator $\mathcal{O}_{\mathrm{ref}} \equiv \vec{a} \cdot \vec{x}_i$. The $E1$ case then follows immediately.

Integration over flux-tube variables gives

$$\langle \chi_1, \pm | \vec{a} \cdot \vec{x}_\pm | \chi_0 \rangle = \pm \frac{1}{\beta_1} (\delta^+ \mathcal{D}^{(1)*}_{\pm +} - \delta^- \mathcal{D}^{(1)*}_{\pm -}), \tag{16}$$

$$\langle \chi_1, \pm | \vec{a} \cdot \hat{z} | \chi_0 \rangle = - \frac{1}{\sqrt{2}\beta_1} (\delta^+ \mathcal{D}^{(1)*}_{0+} - \delta^- \mathcal{D}^{(1)*}_{0-}), \tag{17}$$

and so, for a transition from a conventional $^1S_0$ state, for example, we have[2]

$$\begin{aligned} &\langle \mathrm{hyb}; \pm, m' | \exp\left[-i\vec{q} \cdot \vec{r} \frac{\mu}{m_Q} \right] \vec{a} \cdot \vec{x}_- | \mathrm{conv}; l = 0 \rangle \\ &= \int d^3\vec{r} \left[R_{\mathrm{hyb}}(r) \sqrt{\frac{3}{4\pi}} \mathcal{D}^{(1)*}_{m', \pm} \right]^* e^{-i\vec{q}\cdot\vec{r}(\mu/m_Q)} \left(-\frac{1}{\beta_1} \right) \\ &\quad \times (\delta^+ \mathcal{D}^{(1)*}_{-+} - \delta^- \mathcal{D}^{(1)*}_{--}) \left[R_{\mathrm{conv}}(r) \frac{1}{\sqrt{4\pi}} \right]. \end{aligned} \tag{18}$$

First expand the exponential in terms of partial-wave angular states, contract together the three $\mathcal{D}$ functions, and integrate $\int d\Omega$, which gives, for the matrix element (see Appendix B),

$$\begin{aligned} &-\frac{1}{\beta_1} \frac{1}{\sqrt{3}} \delta_{m', -1} \left[\left({}_f\langle j_0 \rangle_i - \frac{1}{2} {}_f\langle j_2 \rangle_i \right) (\delta^+ - \delta^-) \right. \\ &\quad \left. - i \frac{3}{2} {}_f\langle j_1 \rangle_i (\delta^+ + \delta^-) \right], \end{aligned}$$

where we now only need to calculate the radial expectation values of the spherical Bessel functions.

In the previous equations the factors $\delta^\pm$ refer to the flux tube polarization transverse to the body vector $\vec{r}$, while the $\delta_{m', \pm 1}$ refers to the meson's total angular momentum projection in the fixed axes $(\hat{x}, \hat{y}, \hat{z})$. The parity eigenstates in the flux tube are given in Ref. [3]. They are linear superpositions of states where the flux tube has polarization ± 1. Following that reference we denote the number of positive or negative helicity phonon modes by $\{n_+, n_-\}$, which for our present purposes will be $\{1,0\}$ or $\{0,1\}$. Parity eigenstates are then the linear superpositions

$$|\mathcal{P} = \pm\rangle \equiv \frac{1}{\sqrt{2}} (|\{1,0\}\rangle \mp |\{0,1\}\rangle).$$

The effect is that when we take expectation values for parity eigenstates, the terms proportional to $(\delta^+ \pm \delta^-)$ will be destroyed for the ''wrong'' parity and amplified by $\sqrt{2}$ for the ''correct'' parity.

This is the source of the extra overall factor of $\sqrt{2}$ in the following expressions for transitions to specific parity eigenstates. With this preamble we now proceed to complete the expression for parity eigenstates.

[2] See [3] for a derivation of the angular dependence of the hybrid wave function.

In the above the argument of Bessel functions is $j_n(-|\vec{q}|r(\mu/m_Q))$. Using $j_n(-x)\equiv(-1)^n j_n(x)$ we can replace the argument of the Bessel functions to be $j_n(|\vec{q}|r(\mu/m_Q))$ and gather together the general structure of the matrix elements for the various polarization states:

$$\langle \text{hyb};\mathcal{P},m'|\exp\left[-i\vec{q}\cdot\vec{r}\frac{\mu}{m_Q}\right]\vec{a}\cdot\vec{x}_\pm|\text{conv};l=0\rangle$$
$$=\pm\frac{1}{\beta_1}\sqrt{\frac{2}{3}}\left\{\delta(\mathcal{P}=+)\left({}_f\langle j_0\rangle_i-\frac{1}{2}{}_f\langle j_2\rangle_i\right)\right.$$
$$\left.\mp\frac{3i}{2}\delta(\mathcal{P}=-)\,{}_f\langle j_1\rangle_i\right\}\delta_{m',\pm1} \tag{19}$$

and

$$\langle \text{hyb};\mathcal{P},m'|\exp\left[-i\vec{q}\cdot\vec{r}\frac{\mu}{m_Q}\right]\vec{a}\cdot\hat{z}|\text{conv};l=0\rangle$$
$$=-\frac{1}{\sqrt{2}\beta_1}\sqrt{\frac{2}{3}}\{\delta(\mathcal{P}=+)({}_f\langle j_0\rangle_i+{}_f\langle j_2\rangle_i)\}\delta_{m',0}. \tag{20}$$

These are the main equations that set the normalization for hybrid excitation involving any operator. To illustrate how they are applied we return to the specific example of $E1$ electromagnetic transitions.

The $E1$ operator is Eq. (15); thus, we simply rescale the above expressions accordingly. Noting that $|\vec{\epsilon}_\pm|/|\vec{x}_\pm|=1/\sqrt{2}$ we have, effectively,

$$\mathcal{O}_{E1}/\mathcal{O}_{\text{ref}}=|\vec{q}|\left(\frac{e_Q}{m_Q}+\frac{e_d}{m_d}\right)\sqrt{\frac{b}{\pi^3}}\beta_1 r.$$

The matrix element for the transition from ${}^1S_0$ to spin-singlet hybrid (1^{++}) then follows upon multiplying this ratio by the reference form (19) (for $\mathcal{P}=+$), in the $|\vec{q}|r\ll1$ limit,

$$\langle \text{hyb};\mathcal{P}=+,m'|\vec{a}\cdot\vec{x}_+|\text{conv};l=0\rangle$$
$$=+\frac{1}{\beta_1}\sqrt{\frac{2}{3}}\delta(\mathcal{P}=+)\,\delta_{m',+1},$$

giving, finally,

$$\mathcal{M}(\text{conv}(0^{-+})\,\gamma\rightleftharpoons\text{hyb}(1^{++}))$$
$$=\left(\frac{e_1}{m_1}+\frac{e_2}{m_2}\right)|\vec{q}|\sqrt{\frac{2b}{3\pi^3}}\delta_{m',+1}$$
$$\times\int r^2\,dr\,R^*_{\text{hyb}}(r)rR_{\text{conv}}(r),$$

which is the form used in Ref. [22].

This applies immediately to the excitation of the hybrid $a_{1H}^\pm$ in $\gamma\pi^\pm\to a_{1H}^\pm$ where there is no spin flip between the spin singlets π and a_{1H}. Note that this transition requires charged states, the neutral modes vanishing in accordance with charge conjugation:

$$\mathcal{M}(\gamma\pi\rightleftharpoons a_{1H})\approx\left(\frac{e_1+e_2}{m_n}\right){}_H\langle r\rangle_\pi|\vec{q}_H|\sqrt{\frac{2b}{3\pi^3}}, \tag{21}$$

$$\mathcal{M}(\gamma\pi\rightleftharpoons b_1)\approx\left(\frac{e_1-e_2}{m_n}\right){}_b\langle r\rangle_\pi|\vec{q}_b|\frac{m_n}{2\sqrt{3}}. \tag{22}$$

So the ratio of widths becomes

$$\frac{\Gamma_{E1}(a_{1H}^+\to\pi^+\gamma)}{\Gamma_{E1}(b_{1Q}^+\to\pi^+\gamma)}$$
$$=\frac{72}{\pi^3}\frac{b}{m_n^2}\left|\frac{{}_H\langle r\rangle_\pi}{{}_b\langle r\rangle_\pi}\right|^2\left[\frac{|\vec{q}_H|^3\exp\left(-\frac{|\vec{q}_H|^2}{8\beta_H^2}\right)}{|\vec{q}_b|^3\exp\left(-\frac{|\vec{q}_b|^2}{8\beta_b^2}\right)}\right], \tag{23}$$

where the factor in square brackets includes the q^3 phase space and a ''typical'' form factor taken from the case of harmonic-oscillator binding [23]. These factors model the nontrivial hybrid meson mass dependence of the width.[3]

Compare the form of the ratio of $E1$ widths (after removing a factor of 9 due to the different charge factors), with the transverse contribution to the elastic charge radius, Eq. (10). In the approximations that we have used here, the $E1$ transitions to the leading states saturate the dipole sum rule.

Our calculation of the relative strengths of the matrix elements for hybrid and conventional $E1$ transitions, Eqs. (21), (22), in the flux-tube model, suggests a way of calculating this more directly in lattice QCD. The essential features of the electromagnetic matrix elements are (i) take an initial charged $\pi^\pm$, (ii) apply an $E1$ transition operator with no spin flip, and (iii) compute matrix element to $J^P=1^+$ final states with G parity $=\pm1$.

The transition to G parity $+1$ is to the conventional spin-singlet axial meson, while that to $G=-1$ is only accessible for the hybrid configuration. If further one calculated $\langle r^2\rangle$ for the $\pi^\pm$, one could assess how well the sum rule is saturated by these states, quantify the ''penalty'' for exciting the gluonic modes or hybrids in general, and potentially assess the role of such configurations in the π wave function.

[3]Keeping the full spherical Bessel functions in the radial overlap gives a form factor very similar to this. Even calculated true to the model, the form factors should be considered to be at best rough guides to the mass dependence especially in regions where the nonrelativistic approximation is failing.

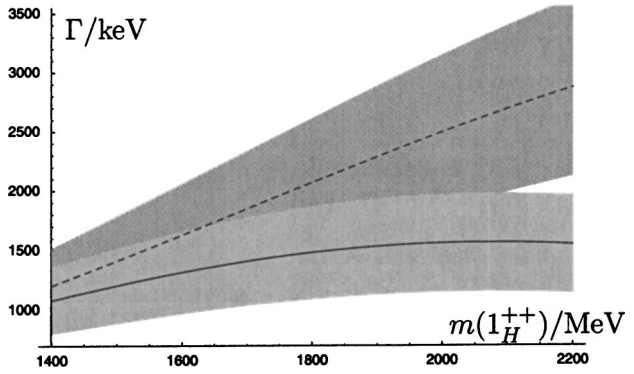

FIG. 2. $E1$ width as a function of 1^{++} hybrid mass. The solid line is for $\beta_\pi = 335$ MeV. The dashed line is for $\beta_\pi = 540$ MeV [24]. The shaded gray areas are the uncertainties due to the error in the experimental rate used as normalization.

C. $E1$ rates

In the Isgur-Paton adiabatic model [3] with a variational harmonic-oscillator solution[4] we obtain $|{}_H\langle r\rangle_\pi / {}_b\langle r\rangle_\pi|^2 \approx 1.0$, so the radial moments do not suppress hybrid production. We follow Ref. [3] and use the standard parameters $b = 0.18\ \mathrm{GeV}^2$, $m_n = 0.33$ GeV so that the prefactor $(72/\pi^3) b/m_n^2 \approx 3.8$ and hence there is no hybrid suppression from the flux-tube dynamics.

Within our variational solution $\beta_H = 255$ MeV, $\beta_b = 281$ MeV, $\beta_\pi = 335$ MeV, so we see the $p=1$ hybrid state being roughly the same size as the $L=1$ conventional state. The main uncertainty is the computed size of the π [23]. Assuming that this hybrid has mass ~ 1.9 GeV [2,3,19] and using the measured width $\Gamma(b_1^+ \to \pi^+ \gamma) = 230 \pm 60$ keV [21] we predict that

$$\Gamma(a_{1H}^+ \to \pi^+ \gamma) = 2.1 \pm 0.9 \ \ \mathrm{MeV}, \tag{24}$$

where the error allows for the uncertainty in β_π [23,24]. We present in Fig. 2 the dependence of the radiative width on the mass of the hybrid.

The equivalent $E1$ process for $S=1$ is $b_{JH} \to \rho\gamma$, where the only difference from the $S=0$ case is the addition of L,S Clebsch-Gordan factors coupling the $Q\overline{Q}$ spin and flux-tube angular momentum to the total J of the hybrid meson in question. As above, the charge conjugation of the initial and final states is the same; thus, $\Delta C = 0$, and the amplitude is proportional to $e_1 + e_2$. Consider absorption of a positive helicity photon. The hybrid state is constructed as

$$|J^{+-}, m_J\rangle = \sum_{m_S, m'} \langle 1m'; 1m_S | J m_J\rangle \frac{1}{\sqrt{2}} \{ |\mathrm{hyb}; +, m'\rangle - |\mathrm{hyb}; -, m'\rangle \} | S=1, m_S\rangle$$

[4]See Appendix D.

TABLE II. Photon-meson-hybrid $E1$ matrix elements: $\mathcal{M} = (e_1/m_1 + e_2/m_2)|\vec{q}|\sqrt{2b/3\pi^3}\,{}_H\langle r\rangle_i$ should be multiplied by the Clebsch-Gordan factor in the second column to give the overall matrix element for a positive helicity photon. The numbers quoted in columns 3 and 4 are $\mathcal{M}/|\vec{q}|$ (10^{-3} GeV^{-1}), evaluated using the results of Appendix D, except those in brackets which use the β values of [24].

State		$u\overline{d}$	$u\overline{s}$
$^1S_0$	$\times 1$	$\gamma\pi^+ \to a_{1H}^+$	$\gamma K^+ \to K_{1AH}^+$
		56 (23)	43 (23)
$^3S_1$	$\times \langle 11; 1m_i | J_H m_H\rangle$	$\gamma\rho^+ \to b_{JH}^+$	$\gamma K^{*+} \to K_{JBH}^+$
		56	43
$^1P_1$	$\times \sqrt{\frac{3}{2}} \langle 11; 1m_i | 1m_H\rangle$	$\gamma b_1^+ \to \rho_H^+$	$\gamma K_{1B}^+ \to K_H^{*+}$
		87	68
^3P_J	$\times \Sigma_{m_L, m_S} \langle 1m_L; 1m_S | J m_J\rangle$	$\gamma a_J^+ \to \pi_{J_H H}^+$	$\gamma K_{JA}^+ \to K_{J_H H}^+$
	$\times \sqrt{\frac{3}{4}} \langle 1m_L + 1; 1m_S | J_H m_H\rangle^*$	87	68

and the matrix element becomes

$$\mathcal{M}(\gamma\rho \rightleftharpoons b_{JH}) = \langle 1+1; 1m_\rho | J m_J\rangle \times \left(\frac{e_1+e_2}{m_n}\right) {}_H\langle r\rangle_\rho |\vec{q}_H| \sqrt{\frac{2b}{3\pi^3}}.$$

We find for $J = 0,1,2$ in this $E1$ limit, normalizing against measured $\Gamma(f_1 \to \rho\gamma)$,

$$\Gamma(b_{JH}^+ \to \rho^+ \gamma) = 2.3 \pm 0.8 \ \mathrm{MeV}, \tag{25}$$

where the error reflects the uncertainties in the conventional $E1$ strength and β_{f_1} and where we have taken $m_H = 1.9$ GeV.

We present in Table II formulas for $E1$ radiative matrix elements between conventional and hybrid states. Of particular interest is the rate of production of the isovector $1^{-+}(\pi_{1H})$ at 1.6 GeV. We use the $E1$ decay of this state to a_2 as an explicit example of the use of Table II. With a positive helicity photon there are three helicity amplitudes, corresponding to $m_J = -2, -1, 0$:

$$\mathcal{M}_{-2} = \sqrt{\frac{3}{4}} \langle 1-1; 1-1 | 2-2\rangle \langle 10; 1-1 | 1-1\rangle \mathcal{M} = \frac{1}{\sqrt{2}} \sqrt{\frac{3}{4}} \mathcal{M},$$

$$\mathcal{M}_{-1} = \sqrt{\frac{3}{4}} (\langle 10; 1-1 | 2-1\rangle \langle 1+1; 1-1 | 10\rangle + \langle 1-1; 10 | 2-1\rangle \langle 10; 10 | 10\rangle) \mathcal{M} = \frac{1}{2} \sqrt{\frac{3}{4}} \mathcal{M},$$

$$\mathcal{M}_0 = \sqrt{\frac{3}{4}}(\langle 1-1;1+1|20\rangle\langle 10;1+1|1+1\rangle + \langle 10;10|20\rangle\langle 1+1;10|1+1\rangle)\mathcal{M} = \frac{1}{2\sqrt{3}}\sqrt{\frac{3}{4}}\mathcal{M},$$

where $\mathcal{M}=|\vec{q}|87\times10^{-3}$ GeV^{-1}. Using Eq. (14) we obtain

$$\Gamma_{E1}(\pi_{1H}\to a_2\gamma) = 4\frac{E_{a_2}}{m_{\pi_{1H}}}|\vec{q}|\frac{1}{3}(|\mathcal{M}_{-2}|^2+|\mathcal{M}_{-1}|^2+|\mathcal{M}_0|^2) = \frac{E_{a_2}}{m_{\pi_{1H}}}|\vec{q}|^3\left(\frac{1}{2}+\frac{1}{4}+\frac{1}{12}\right) \times(87\times10^{-3}\ \text{GeV}^{-1})^2,$$

so that for a π_{1H} at 1.6 GeV the width is $\sim$90 keV. Given that a_2 exchange is suppressed relative to f_2 in photoproduction of $I=1$ states, this is unlikely to be a major production route in $\gamma p\to\pi_{1H}n$. Pion exchange provides an opportunity via the $M1$ multipole but this goes beyond our present discussion. If calculated via the vector dominance model (VDM) from the $\pi_{1H}\to\pi\rho$ rate, where the photon-rho flux tube is excited by a "pion current," we find [25] $\Gamma(\pi_{1H}\to\gamma\pi)\sim200$ keV which is similar to that found in [11].

A state potentially interesting in heavy flavor decay (see next section) is the axial hybrid kaon; we find that this state has an $E1$ width to $K\gamma$ of 300–1000 keV (assuming mass $\sim$2 GeV). This state could be seen in photoproduction by looking in the $K\pi\pi\Lambda$ end state.

Note that these $E1$ transitions are only possible with charge exchange and so cannot occur between flavorless states. In particular they are absent for $c\bar{c}$ and $b\bar{b}$. Thus, for example, the transitions $\psi(3685)\to\gamma\chi_J$ can receive no contribution from any hybrid component of the $\psi(3685)$ wave function (assuming here that the χ_{JH} states are $\gg4$ GeV in mass and so do not mix measurably into the $c\bar{c}$ states.)

This illustrates the principle for calculating matrix elements for hybrid excitation by currents. We can extend this now to vector and axial currents of arbitrary polarization and apply to the production of hybrid mesons in the weak decays of heavy flavors. This requires a nonrelativistic decomposition of the currents (Appendix A); then, we identify the terms linear in $\vec{a}$ which can cause transitions between conventional and first excited hybrids. Finally all one then needs to do is to read off the relevant operator, scale by the reference operator as above, and determine the relevant matrix elements.

IV. HEAVY FLAVOR DECAYS TO HYBRID MESONS

In the first half of this paper we have described the method of calculation used to compute amplitudes for processes involving a hybrid meson, a conventional meson, and a current by considering the specific example of hybrid meson radiative decay. The results obtained are applicable to the forthcoming hybrid photoproduction experiments at Jefferson Lab [26].

We will now use the same techniques to calculate the rate of production of hybrids in heavy flavor decays. Such a calculation is timely in view of the orders of magnitude increase in statistics on a wide range of exclusive decay channels anticipated at present and upgraded B and charm factories. We will consider in particular the supposed excess of events in the inclusive decay $B\to J/\psi X$ at low J/ψ momentum [13] as this may have an explanation in terms of hybrid kaon production.

In Tables III and IV we identify the exclusive channels in which hybrids may be clearly observed. We begin by outlining the model used to describe the nonleptonic weak decay process.

TABLE III. BR($\bar{B}^0\to\pi^- D_H^+(J^{P(C)})$).

m_{D_H} (GeV)	2.7	3.0	3.3	
$\langle j_0\rangle$	0.62	0.65	0.67	
$\langle j_1\rangle$	0.24	0.22	0.21	
$\langle j_2\rangle$	0.06	0.05	0.04	
$1^{+(+)}$	6.1	4.5	3.0	$\times10^{-4}$
$1^{-(-)}$	0	0	0	
$0^{-(+)}$	3.1	2.5	1.9	$\times10^{-7}$
$1^{+(-)}$	1.3	1.3	1.2	$\times10^{-6}$
$2^{-(+)}$	1.6	1.3	0.9	$\times10^{-7}$
$0^{+(-)}$	3.0	2.3	1.6	$\times10^{-4}$
$1^{-(+)}$	4.9	3.6	2.5	$\times10^{-6}$
$2^{+(-)}$	3.3	2.3	1.5	$\times10^{-4}$

A. Naive factorization model

The matrix element for decays $B\to M_1M_2$ will be written in the generic form (see, e.g., Ref. [27])

TABLE IV. BR($B^+\to J/\psi K_H^+(J^{P(C)})$). The subscripts are the longitudinal rate fractions.

$m_{K_H^-}$ (GeV)	1.8	2.0	2.1	
$\langle j_0\rangle$	0.54	0.63	0.69	
$\langle j_1\rangle$	0.25	0.20	0.14	
$\langle j_2\rangle$	0.08	0.04	0.02	
$1^{+(+)}$	$2.9_{92\%}$	$1.2_{79\%}$	$0.6_{60\%}$	$\times10^{-4}$
$1^{-(-)}$	1.3	0.6	0.2	$\times10^{-5}$
$0^{-(+)}$	5.7	2.8	1.0	$\times10^{-6}$
$1^{-(+)}$	$6.0_{32\%}$	$2.5_{19\%}$	$0.8_{10\%}$	$\times10^{-6}$
$2^{-(+)}$	$7.0_{41\%}$	$3.5_{40\%}$	$1.3_{40\%}$	$\times10^{-6}$
$0^{+(-)}$	9.8	4.1	1.4	$\times10^{-5}$
$1^{+(-)}$	$3.1_{5\%}$	$1.7_{11\%}$	$0.9_{18\%}$	$\times10^{-4}$
$2^{+(-)}$	$2.9_{39\%}$	$1.1_{39\%}$	$0.3_{39\%}$	$\times10^{-4}$

$$\langle M_1 M_2|\mathcal{H}_{\rm eff}|B\rangle = \frac{G_F}{\sqrt{2}} V_{q_1' b} V_{q_2' q_2} \mathcal{O}, \tag{26}$$

with

$$\mathcal{O} = a_1(\mu)\langle M_1|\bar{q}_1'(V-A)b|B\rangle\langle M_2|\bar{q}_2(V-A)q_2'|0\rangle + a_2(\mu)\langle M_2|\bar{q}_2(V-A)b|B\rangle\langle M_1|\bar{q}_1'(V-A)q_2'|0\rangle. \tag{27}$$

The model arises from performing the QCD renormalization of the weak interaction, supposing that one of the mesons is created from the vacuum by a current with the same quantum numbers. Final state interactions are ignored. a_1, a_2 are considered as phenomenological parameters determined by fitting to known conventional decay rates and not as the Wilson coefficients they would be in the strict theory.

Decays proceeding by the first term only are labeled "class I," an example being $\bar{B}^0 \to \pi^- D^{(*)+}$ which in this model has amplitude

$$\frac{G_F}{\sqrt{2}} V_{bc} V_{ud} a_1 \langle \pi^-|\bar{d}A_\mu u|0\rangle\langle D^{(*)+}|\bar{c}(V^\mu - A^\mu)b|\bar{B}^0\rangle. \tag{28}$$

The pion creation current is conventionally parametrized by $\langle \pi^-(q)|\bar{d}A_\mu u|0\rangle \equiv i f_\pi q_\mu$ and we compute the hadronic matrix element using our nonrelativistic quark-flux-tube model.

Decays proceeding only by the second term in Eq. (27) are labeled "class II" or "color-suppressed" and include the well tested channel $B^+ \to K^{(*)+} J/\psi$ with amplitude

$$\frac{G_F}{\sqrt{2}} V_{bc} V_{cs} a_2 \langle J/\psi|\bar{c}V_\mu c|0\rangle\langle K^{(*)+}|\bar{s}(V^\mu - A^\mu)b|B^+\rangle, \tag{29}$$

where the J/ψ current has Lorentz decomposition $\langle J/\psi(q,\epsilon)|\bar{c}V_\mu c|0\rangle \equiv \epsilon_\mu^* f_\psi m_\psi$.

Models of this type are more thoroughly discussed in [27] where they are demonstrated to successfully predict weak decay rates of the B meson to a wide range of conventional exclusive channels.

We use meson state normalizations as in [28] such that a factor $\sqrt{4 m_B m_M}$ appears in all hadronic matrix elements (where M is the meson not created from the vacuum); then, decay widths are written in the following manner:

$$\Gamma(\bar{B}^0 \to \rho^- D^{+(*)}) = \frac{G_F^2}{16\pi} \frac{|\vec{q}|}{m_B^2} |V_{bc} V_{ud}|^2 |a_1|^2 \sum_{\rm helicities} |\mathcal{M}|^2, \tag{30}$$

where $\mathcal{M} = \langle \rho^-|\bar{d}V_\mu u|0\rangle\langle D^{(*)+}|\bar{c}(V^\mu - A^\mu)b|\bar{B}^0\rangle$ and where to be specific we have shown the case of the class I decay to a conventional vector. We will use $a_1 = 1.05$, $a_2 = 0.25$ for all B decays; these numbers are compatible with those in [27] and give a good fit to the conventional decays.

B. Application to *B* decays producing hybrid mesons

In this section we extend the established model described above to include hybrids in the end state, in much the same was as we extended the conventional radiative decay formalism previously. We simply include the additional flux-tube transverse degree of freedom, $\vec{a}$, in the currents and wave functions. As in the radiative case this both modifies conventional decay rates (by changing the charge radius or Isgur-Wise function as detailed in Sec. III) and allows for hybrid excitation.

Previous models of hybrid production in this type of process [29,30] have assumed that hybrids are created by a color-octet current with some undetermined strength. The Isgur-Paton flux-tube model has the gluonic field in a color singlet and as such we will create hybrids using the same current that creates conventional mesons.

When considering weak decays of heavy-light systems we use the following form of the quark position vector:

$$\vec{r}_{Q(d)} = \vec{R} \pm \vec{r}\frac{\mu}{m_{Q(d)}} - \vec{a}\frac{2\beta_1 r}{m_Q + m_d}\sqrt{\frac{2b}{\pi^3}}.$$

This differs slightly from the form used previously, Eq. (12). It has the advantage that under a finite change in heavy quark mass (i.e., a flavor changing transition) $\vec{r}$, which here is the interquark separation vector, and $\vec{a}_p$ are unchanged. For details see [31].

C. *B* decays to hybrid plus conventional pseudoscalar

The matrix element for such a decay is

$$\mathcal{M}(B \to PH) = i f_P q \cdot \langle H|(V-A)|B\rangle.$$

Examples include $\bar{B}^0 \to \pi^- D_H^+$ (class I) and $\bar{B}^0 \to D^0 n\bar{n}_H$ (class II).[5] Thus to compute the branching ratio for $\bar{B}^0 \to \pi^- D_H^+$ we need the values of the operators $q\cdot A$ and $q\cdot V$ between B and D_H wave functions. In Appendix A we compute the terms in the nonrelativistic reduction of V_μ and A_μ that are linear in $\vec{a}$ and which therefore can induce transitions between conventional and hybrid mesons.

We find, for the maximally parity violating current,

[5]Recent theoretical work [32] suggests that naive factorization can be a poor approximation for processes $\bar{B}^0 \to D^0 +$ light hadrons.

$$q\cdot V_H = e^{-i\vec{q}\cdot\vec{r}m_d/m_D}\sqrt{\frac{2b}{\pi^3}}\beta_1|\vec{q}| \times\left\{ i\vec{a}\cdot\hat{z}\left[\frac{\pi}{2m_b}\left(1+\frac{m_b}{m_c}+\frac{|\vec{q}|}{2m_c}\right) +|\vec{q}|\frac{2r}{m_D}\left(1+\frac{|\vec{q}|}{2m_c}\right)\right] +\vec{\sigma}\cdot\hat{z}\wedge\vec{a}\frac{\pi}{2m_b}\left(-1+\frac{m_b}{m_c}-\frac{|\vec{q}|}{2m_c}\right)\right\}, \quad (31)$$

and for the parity conserving current,

$$q\cdot A_H = e^{-i\vec{q}\cdot\vec{r}(m_d/m_D)}\sqrt{\frac{2b}{\pi^3}}\beta_1|\vec{q}| \times\left\{ -i\vec{\sigma}\cdot\vec{a}\frac{\pi}{2m_b}\left(1+\frac{m_b}{m_c}+\frac{|\vec{q}|}{2m_c}\right) -i|\vec{q}|\sigma_z\vec{a}\cdot\hat{z}\frac{2r}{m_D}\left(1+\frac{|\vec{q}|}{2m_c}\right)\right\}, \quad (32)$$

having approximated $q^2=m_\pi^2\approx 0$, as appropriate for B decays.

1. Spin-singlet hybrids, $D_H(1^{\pm(\pm)})$

Since $\langle\vec{\sigma}\rangle=0$ for the transition to a hybrid where the $q\bar{q}$ spins are coupled to $S=0$, the parity conserving current, Eq. (32), plays no role here. Nonvanishing contributions come entirely from the first term of the parity violating current, Eq. (31). We thus have a matrix element

$$\mathcal{M}(\bar{B}^0\to\pi^- D_H^+(S=0)) = if_\pi\langle D_H|e^{-i\vec{q}\cdot\vec{r}(m_d/m_D)} \times\sqrt{\frac{2b}{\pi^3}}\beta_1|\vec{q}|\vec{a}\cdot\hat{z}\left[\frac{\pi}{2m_b}\left(1+\frac{m_b}{m_c}+\frac{|\vec{q}|}{2m_c}\right) +|\vec{q}|\frac{2r}{m_D}\left(1+\frac{|\vec{q}|}{2m_c}\right)\right]|B\rangle.$$

The integrals over $\vec{a}$ and angles θ,ϕ are performed in Appendix B, and we take the result, Eq. (20),

$$\langle \mathrm{hyb};\mathcal{P},m'|\exp\left[-i\vec{q}\cdot\vec{r}\frac{\mu}{m_Q}\right]\vec{a}\cdot\hat{z}|\mathrm{conv};l=0\rangle = -\frac{1}{\sqrt{2}\beta_1}\sqrt{\frac{2}{3}}\delta(\mathcal{P}=+)(\langle j_0\rangle+\langle j_2\rangle)\,\delta_{m',0},$$

where in the current example the argument of the spherical Bessel functions is $|\vec{q}|r(m_d/(m_d+m_c))$. Thus we have the matrix elements

$$\mathcal{M}(\bar{B}^0\to\pi^- D_H^+(1^{-(-)}))=0, \quad (33)$$

$$\mathcal{M}(\bar{B}^0\to\pi^- D_H^+(1^{+(+)})) = -if_\pi\sqrt{4m_Bm_D}\sqrt{\frac{2b}{3\pi^3}}|\vec{q}| \times\left\{\frac{\pi}{2m_b}\left(1+\frac{m_b}{m_c}+\frac{|\vec{q}|}{2m_c}\right) \times(\langle j_0\rangle+\langle j_2\rangle)+\frac{6}{m_d}\left(1+\frac{|\vec{q}|}{2m_c}\right)\langle j_1\rangle\right\}. \quad (34)$$

That the $1^{-(-)}$ amplitude is zero was to be expected as one cannot maximally violate parity and conserve angular momentum in a process $0^-\to 1^-0^-$ in any partial wave, whereas the $1^{+(+)}$ amplitude is nonzero as $0^-\to 1^+0^-$ in a P wave respects the symmetries.

2. Spin-triplet hybrids, $D_H(J^{\pm(\mp)})$

To excite spin-triplet hybrids we require operators linear in $\vec{\sigma}$ and $\vec{a}$, which feature in both $q\cdot A$ and $q\cdot V$, Eqs. (31), (32).

For simplicity in presentation we shall define $\rho_\pm \equiv(\pi/2m_b)(1\pm m_b/m_c+|\vec{q}|/2m_c)$. We can decompose $\vec{\sigma}\cdot\hat{z}\wedge\vec{a}=(1/2i)(\sigma_+\vec{a}\cdot\vec{x}_- -\sigma_-\vec{a}\cdot\vec{x}_+)$ and $\vec{\sigma}\cdot\vec{a}=\frac{1}{2}(\sigma_+\vec{a}\cdot\vec{x}_-+\sigma_-\vec{a}\cdot\vec{x}_+)+\sigma_z\vec{a}\cdot\hat{z}$, where $\sigma_\pm,\sigma_z$ are normalized such that

$$\langle S=1,m_S|^{\sigma_\pm}_{\sigma_z}|S=0\rangle=\begin{bmatrix}\mp\sqrt{2}\,\delta(m_S,\pm1)\\ \delta(m_S,0)\end{bmatrix}.$$

The $S=1$ of the quarks and $L=1$ of the flux tube combine together to give the J of the hybrid meson, with the appropriate Clebsch-Gordan coefficient $\langle 1m_L;1m_S|Jm_J\rangle$. Performing the integrations over $\vec{a}$ and angles θ,ϕ as in Appendix B gives, for the parity violating current,

$$\mathcal{M}_{q\cdot V}=-f_\pi\sqrt{4m_Bm_D}\sqrt{\frac{2b}{3\pi^3}}|\vec{q}|\rho_-\sum_{m_L,m_S}\langle 1m_L;1m_S|Jm_J\rangle \begin{Bmatrix}\delta(\mathcal{P}=+)\left(\langle j_0\rangle-\frac{1}{2}\langle j_2\rangle\right)(\delta_{m_L,-1}\delta_{m_S,+1}-\delta_{m_L,+1}\delta_{m_S,-1})\\ +\delta(\mathcal{P}=-)\frac{3i}{2}\langle j_1\rangle(\delta_{m_L,-1}\delta_{m_S,+1}+\delta_{m_L,+1}\delta_{m_S,-1})\end{Bmatrix}. \quad (35)$$

The pattern of amplitudes for various J^{PC} follows from the combination of Clebsch-Gordan coefficients:

$$\delta(\mathcal{P}=+)\left(\langle j_0\rangle-\frac{1}{2}\langle j_2\rangle\right)[\langle 1-1;1+1|J0\rangle$$
$$-\langle 1+1;1-1|J0\rangle]+\delta(\mathcal{P}=-)\frac{3i}{2}\langle j_1\rangle$$
$$\times[\langle 1-1;1+1|J0\rangle+\langle 1+1;1-1|J0\rangle].$$

Thus we find, for the maximally parity violating current,

$$\mathcal{M}_{q\cdot V}\begin{pmatrix}0^{+(-)}\\1^{-(+)}\\2^{+(-)}\end{pmatrix}=0,$$

$$\mathcal{M}_{q\cdot V}\begin{pmatrix}0^{-(+)}\\1^{+(-)}\\2^{-(+)}\end{pmatrix}=-\sqrt{4m_Bm_D}\sqrt{\frac{2b}{3\pi^3}}f_\pi|\vec{q}|\rho_-$$
$$\times\begin{Bmatrix}\frac{i}{\sqrt{3}}\langle j_1\rangle\\-\sqrt{2}\left(\langle j_0\rangle-\frac{1}{2}\langle j_2\rangle\right)\\\frac{i}{\sqrt{6}}\langle j_1\rangle\end{Bmatrix}. \quad (36)$$

An exactly analogous process for the parity conserving current gives

$$\mathcal{M}_{q\cdot A}\begin{pmatrix}0^{-(+)}\\1^{+(-)}\\2^{-(+)}\end{pmatrix}=0,$$

$$\mathcal{M}_{q\cdot A}\begin{pmatrix}0^{+(-)}\\1^{-(+)}\\2^{+(-)}\end{pmatrix}$$
$$=\sqrt{4m_Bm_D}\sqrt{\frac{2b}{3\pi^3}}f_\pi|\vec{q}|\left(\frac{\rho_+}{\sqrt{2}}\begin{Bmatrix}\sqrt{6}\langle j_0\rangle\\-3i\langle j_1\rangle\\-\sqrt{3}\langle j_2\rangle\end{Bmatrix}\right.$$
$$\left.+\frac{2\sqrt{3}}{m_d}\left(1+\frac{|\vec{q}|}{2m_c}\right)\langle j_1\rangle\begin{Bmatrix}1\\0\\-\sqrt{2}\end{Bmatrix}\right). \quad (37)$$

As in the spin-singlet case we can understand the zero values as originating in the need for angular momentum conservation while applying the appropriate parity selection rule.

3. Numerical estimates

The model parameters and variational wave functions used to evaluate the radial matrix elements $\langle D_H|j_L|B\rangle$ are described in Appendix D. We obtain the following results for the branching fractions of the $\bar{B}^0$ meson to the exclusive channel $D_H^+(J^{P(C)})\pi^-$, presented in Table III.

While these are the decays in which the naive factorization approximation is most likely to be correct they are not ideal for hybrid hunting: the D mesons are not eigenstates of C and as such cannot have ''exotic'' quantum numbers, the smoking-gun signature for a hybrid. However, the fact that for a given $J^{P(C)}$ the hybrid and conventional states have $q\bar{q}$ coupled to $S=0(1)$ and $S=1(0)$, respectively, can lead to selection guides. This has been noted already for hadronic processes [5,23]. We shall see that there are further examples in B decays.

The class II decay $\bar{B}^0\to D^0(n\bar{n})_H$, by contrast, can produce exotic quantum numbered hybrids and is not suppressed by any small Cabibbo-Kobayashi-Maskawa (CKM) matrix elements. Unfortunately there are problems both with factorization [32] and with our model formulation when applied to this decay. Our model has form factors obtained from the simple wave function overlaps $\langle H|j_L|B\rangle$, and although these are reasonable at small $|\vec{q}|$ where everything is nonrelativistic, they are at best a qualitative guide as the phase space rises. Such subtleties are discussed in [33] where a better fit to the spectrum of semileptonic B decays is found using a power law form factor in contrast to the ''polynomial times exponential'' form that we have used. To reduce the uncertainty we calculate the ratio of hybrid production and conventional (known) rates, for which much of the form factor dependence cancels out. Thus, for example, if we propose that there is a 1^{-+} hybrid at 1600 MeV, we predict that it will have a branching fraction a little smaller than that of $\bar{B}^0\to D^0(\rho,\omega)$—i.e., $O(10^{-5})$. Here $(0,2)^{+-}$ exotics have potentially even larger rates provided that they have masses somewhat below 3 GeV.

In addition to B-meson decays, this formalism can equally well be applied to D and D_s decays, though the factorized model may not be as accurate here. There is some possibility of producing exotic hybrids in the Cabibbo-suppressed decay $D^0\to\pi^+(n\bar{n})_H^-$ if the hybrid is light enough, similarly in the channel $D_s\to\pi^+(s\bar{s})_H$. The numerical branching ratios for these processes are strongly dependent on the hybrid mass as they are so close to kinematic threshold. The candidate 1^{-+} state at 1600 MeV has a branching ratio in this decay of $O(10^{-7})$ principally because it is produced in a P wave with a very small $|\vec{q}|$.

D. *B* decays to hybrid plus conventional vector

The matrix element $\mathcal{M}(B\to VH)=m_Vf_V\epsilon_\mu^*\langle H|(V-A)^\mu|B\rangle$, where ϵ_μ is the vector meson polarization. We thus have a set of amplitudes depending upon the helicity of the vector. Examples of this type of decay include $\bar{B}^0\to\rho^-D^{(*)+}$ (class I) and the well-tested decay $B^+\to J/\psi K^{(*)+}$ (class II).

As discussed in Sec. II, the $|\mathcal{M}|^2$ for the weak transition $B\to\psi K_H(1^+)$ is expected to have strength $\sim$13% relative to its ''conventional'' counterpart $B\to\psi K(1^+)$. Empirically

$B^+ \to \psi K(1^+)(1280)$ is the single largest mode in $B^+ \to \psi X$ with BR$=(1.8\pm 0.5)\times 10^{-3}$ while $B^+ \to \psi K(1^+)(1400) \leqslant 0.5\times 10^{-3}$. These rates involve both parity conserving (vector) and violating (axial) contributions and their relative strengths depend on the mixing between the $^3P_1$ and $^1P_1$ basis states. These rates would lead one to expect an order of magnitude BR for $B^+ \to \psi K_H(1^+) \geqslant 10^{-4}$. This has been reported by us in Ref. [22]. Here we illustrate the calculation.

1. Spin-singlet hybrids

As previously we select the terms in the hybrid currents (Appendix A) independent of $\vec{\sigma}$, for which we find terms in both V_H^μ and A_H^μ. We compute separately the amplitudes for longitudinal and transverse J/ψ.

a. Longitudinal J/ψ and $K_H(1^+)$. For a longitudinal J/ψ, $\epsilon_\psi^\mu = (|\vec{q}|, 0_\perp, E_\psi)/m_\psi$ and so

$$\mathcal{M}_L = f_\psi \langle K_H | |\vec{q}| V_H^0 - E_\psi V_H^3 | B \rangle,$$

since only $A_{H\perp}$ are nonzero for spin singlets. Using the overlaps in Eq. (20) gives

$$\mathcal{M}_L = -i f_\psi \delta(\mathcal{P}=+)\,\delta_{m',0} \sqrt{\frac{2b}{3\pi^3}} \sqrt{4 m_B m_K} \times \left\{ \frac{6|\vec{q}|}{m_d} \left(1 + \frac{E_\psi}{2m_s}\right) \langle j_1 \rangle + \frac{\pi}{2m_b} \left[\frac{|\vec{q}|^2}{2m_s} + E_\psi \left(\frac{m_b}{m_s} + 1 \right) \right] (\langle j_0 \rangle + \langle j_2 \rangle) \right\}. \quad (38)$$

Thus only the positive parity state is produced; there is no longitudinally polarized $K_H(1^{-(-)})$.

b. Transverse J/ψ and $K_H(1^{\pm(\pm)})$. For transverse polarization $\epsilon_\psi^{*\mu} = (0, \vec{\epsilon}^*)$ and $\vec{\epsilon}^* = \mp(1, \mp i, 0)/\sqrt{2}$. Both vector and axial can now contribute. The vector current leads to a matrix element

$$\mathcal{M}_\pm^V = i f_\psi m_\psi \sqrt{4 m_B m_K} \sqrt{\frac{2b}{3\pi^3}} \frac{\pi}{2m_b} \left(\frac{m_b}{m_s} + 1 \right) \delta_{m',\pm 1} \times \left\{ \delta(\mathcal{P}=+) \left(\langle j_0 \rangle - \frac{1}{2} \langle j_2 \rangle \right) \pm \delta(\mathcal{P}=-) \frac{3i}{2} \langle j_1 \rangle \right\} \quad (39)$$

and the axial current to

$$\mathcal{M}_\pm^A = \pm i f_\psi m_\psi \sqrt{4 m_B m_K} \sqrt{\frac{2b}{3\pi^3}} \frac{\pi}{2m_b} \frac{|\vec{q}|}{2m_s} \delta_{m',\pm 1} \times \left\{ \delta(\mathcal{P}=+) \left(\langle j_0 \rangle - \frac{1}{2} \langle j_2 \rangle \right) \pm \frac{3i}{2} \delta(\mathcal{P}=-) \langle j_1 \rangle \right\}. \quad (40)$$

Hence the V_μ and A_μ transitions combine to give the total matrix element for the transition to $1^{+(+)}$:

$$\mathcal{M}_\pm^{V-A}(1^{+(+)}) = i f_\psi m_\psi \sqrt{4 m_B m_K} \sqrt{\frac{2b}{3\pi^3}} \frac{\pi}{2m_b} \times \left\{ \langle j_0 \rangle - \frac{1}{2} \langle j_2 \rangle \right\} \delta_{m',\pm 1} \left[\left(1 + \frac{m_b}{m_s} \right)_{(V)} \mp \left(\frac{|\vec{q}|}{2m_s} \right)_{(A)} \right]. \quad (41)$$

The transition to $1^{-(-)}$ has the same structure apart from the partial wave contributing as j_1 and reads

$$\mathcal{M}_\pm^{V-A}(1^{-(-)}) = -i f_\psi m_\psi \sqrt{4 m_B m_K} \sqrt{\frac{2b}{3\pi^3}} \frac{\pi}{2m_b} \left\{ \frac{3i}{2} \langle j_1 \rangle \right\} \delta_{m',\pm 1} \times \left[\left(1 + \frac{m_b}{m_s} \right)_{(V)} \mp \left(\frac{|\vec{q}|}{2m_s} \right)_{(A)} \right]. \quad (42)$$

We see that for each of these transitions, the vector current dominates. Hence we may anticipate that the transition to $K_H(1^+)$ will be relatively large because the dominant $\langle V_\mu \rangle$ contributes in S wave; by contrast, $K_H(1^-)$ receives its S wave from the $|\vec{q}|/m_b$-suppressed $\langle A_\mu \rangle$ while the vector current contributes to P waves. Explicit calculation, below, confirms this.

c. Longitudinal to transverse ratio. The 1^- hybrid is produced in transverse polarization only. For the 1^+ hybrid both transverse and longitudinal polarizations are possible. Compare the longitudinal matrix element, Eq. (38), with the transverse equation (41) and remove common factors [$A = f_\psi (\sqrt{2b/3\pi^3}) \sqrt{4 m_B m_K}$]:

$$|\mathcal{M}_L| = A \left\{ \frac{6|\vec{q}|}{m_d} \left(1 + \frac{E_\psi}{2m_s}\right) \langle j_1 \rangle + \frac{\pi}{2m_b} \left[\frac{|\vec{q}|^2}{2m_s} + E_\psi \left(\frac{m_b}{ms} + 1 \right) \right] (\langle j_0 \rangle + \langle j_2 \rangle) \right\},$$

$$|\mathcal{M}_{T(\pm)}| = A m_\psi \frac{\pi}{2m_b} \left\{ \langle j_0 \rangle - \frac{1}{2} \langle j_2 \rangle \right\} \times \left[\left(1 + \frac{m_b}{m_s} \right)_{(V)} \mp \left(\frac{|\vec{q}|}{2m_s} \right)_{(A)} \right].$$

Before taking the ratio, consider the actual values of the parameters. For a 1.9 GeV kaon hybrid we have $|\vec{q}| = 0.83$ GeV; thus, $|\vec{q}|/2m_s \approx 0.8$ is negligible next to $(1 + m_b/m_s) \approx 10.5$. The J/ψ is moving nonrelativistically such that for this $|\vec{q}|$, $E_\psi \approx m_\psi$ is good. Using our variational wave functions (Appendix D) we find $\langle j_0 \rangle \approx 0.58$, $\langle j_1 \rangle \approx 0.23$, and $\langle j_2 \rangle \approx 0.06$, so we can safely neglect $\langle j_2 \rangle$. Thus we find

$$\left|\frac{\mathcal{M}_L}{\mathcal{M}_T}\right| \approx 1+\frac{12}{\pi}\frac{m_b}{m_\psi}\frac{|\vec{q}|}{m_d}\left(\frac{1+m_\psi/2m_s}{1+m_b/m_s}\right)\frac{\langle j_1\rangle}{\langle j_0\rangle} \approx 3.4,$$

which leads to a longitudinal width fraction

$$\%\Gamma_L \equiv 100\frac{\Gamma_L}{\Gamma_L+\Gamma_{T(+)}+\Gamma_{T(-)}} \approx 100\left(1+\left|\frac{\mathcal{M}_T}{\mathcal{M}_L}\right|^2\right)^{-1} \approx 90\%.$$

This number should not be taken too seriously, however. It has proved difficult to accommodate the measured value of the longitudinal width fraction of $B^+ \to J/\psi K^{*+}$ within factorized models and this failure may signal the limitations of this simplistic model.

2. Spin-triplet hybrids

Considering the terms in Eqs. (A3),(A5),(A7),(A9) linear in $\vec{\sigma}$ yields the matrix elements

$$\mathcal{M}_L\begin{pmatrix}0^{+(-)}\\1^{-(+)}\\2^{+(-)}\end{pmatrix} = -if_\psi\sqrt{4m_Bm_K}\sqrt{\frac{2b}{\pi^3}}\frac{1}{3}\left(\frac{6}{m_d}\langle j_1\rangle\left(E_\psi+\frac{|\vec{q}|^2}{2m_s}\right)\begin{Bmatrix}-1\\0\\\sqrt{2}\end{Bmatrix}+3|\vec{q}|\frac{\pi}{2m_b}\left(\frac{m_b}{m_s}+1+\frac{E_\psi}{2m_s}\right)\begin{Bmatrix}-\langle j_0\rangle\\ i\sqrt{\frac{3}{2}}\langle j_1\rangle\\ \frac{1}{\sqrt{2}}\langle j_2\rangle\end{Bmatrix}\right), \tag{43}$$

$$\mathcal{M}_L\begin{pmatrix}0^{-(+)}\\1^{+(-)}\\2^{-(+)}\end{pmatrix} = f_\psi\sqrt{4m_Bm_K}\sqrt{\frac{2b}{\pi^3}}E_\psi\frac{\pi}{2m_b}\left(\frac{m_b}{m_s}-1-\frac{|\vec{q}|^2}{2m_sE_\psi}\right)\begin{Bmatrix}\langle j_1\rangle\\ -i\sqrt{\frac{2}{3}}\left(\langle j_0\rangle-\frac{1}{2}\langle j_2\rangle\right)\\ \frac{1}{\sqrt{2}}\langle j_1\rangle\end{Bmatrix}, \tag{44}$$

$$\mathcal{M}_\pm\begin{pmatrix}1^{+(-)}\\2^{+(-)}\end{pmatrix} = if_\psi\sqrt{4m_Bm_K}\sqrt{\frac{2b}{\pi^3}}\frac{1}{\sqrt{6}}m_\psi\left(\frac{6}{m_d}\langle j_1\rangle\left(1\mp\frac{|\vec{q}|}{2m_s}\right)\begin{Bmatrix}\pm1\\1\end{Bmatrix}-\frac{\pi}{2m_b}\left(\frac{m_b}{m_s}-1\pm\frac{|\vec{q}|}{2m_s}\right)\begin{Bmatrix}2\langle j_0\rangle+\frac{1}{2}\langle j_2\rangle\\ \pm\frac{3}{2}\langle j_2\rangle\end{Bmatrix}\right), \tag{45}$$

$$\mathcal{M}_\pm\begin{pmatrix}1^{-(+)}\\2^{-(+)}\end{pmatrix} = f_\psi\sqrt{4m_Bm_K}\sqrt{\frac{2b}{\pi^3}}\sqrt{\frac{3}{8}}m_\psi\frac{\pi}{2m_b}\left(\frac{m_b}{m_s}-1\pm\frac{|\vec{q}|}{2m_s}\right)\langle j_1\rangle\begin{Bmatrix}\pm1\\1\end{Bmatrix}. \tag{46}$$

We can use these matrix elements in the width formula

$$\Gamma(B^+\to J/\psi K_H^+(J^{P(C)})) = \frac{G_F^2}{16\pi}\frac{|\vec{q}|}{m_B^2}|V_{bc}V_{cs}|^2|a_2|^2\sum_{+,-,L}|\mathcal{M}|^2$$

to compute the branching fractions.

3. Numerical estimates

We explicitly evaluate branching fractions and longitudinal rate fractions for the exclusive channel $B^+\to J/\psi K_H^+$ using the parameters and wave functions given in Appendix D, the results being presented in Table IV.

While fine details of the model may be questioned, the $O(10^{-4})$ branching ratio to the hybrids with positive parity appears robust and accessible to experiment. It is intriguing therefore that there is an unexplained enhancement at low q_ψ, corresponding to high mass K systems, of this magnitude [13]. While suggestive, it would be premature to claim this as evidence for hybrid production. Radial excitations of the $K(1^+)$ are expected in this region, and in the ISGW [28] model, extended to exclusive hadronic decays and assuming standard factorization arguments [27], we find these to have BR$\sim 10^{-4}$, though slightly less than the hybrid.

Other conventional strange mesons in this mass range are likely to be suppressed due to their high angular momenta, which give powerful orthogonality suppressions at small $|\vec{q}|$. It is the S-wave character of the hybrid and axial production

that drives their significant production rates.

The channel $\bar{B}^0 \to D^{0*}(n\bar{n})^0_H$, while suffering the same theoretical problems as $\bar{B}^0 \to D^0 n\bar{n}^0_H$ considered earlier, is not in principle suppressed by any small numbers. CLEO II has observed events $\bar{B}^0 \to D^{0*}\pi^+\pi^-\pi^+\pi^-$ [34] which is a possible end state for light quark hybrids decaying via $a_1^{\pm}\pi^{\mp}$ for example. According to the flux-tube breaking model of hybrid hadronic decays [5] isovector 2^{+-},1^{+-},0^{+-},1^{--} and isoscalar 1^{-+},1^{++} hybrids have large branching ratios to $a_1\pi$.

V. DISCUSSION

The results of this paper suggest that the flux tube can be excited without undue penalty. The physics assumes that a flux tube is indeed formed, and if subsequent lattice studies should confirm that the 1 fm length scale of confinement is intermediate between that of perturbative or baglike gluonic fields and a fully formed flux tube, then some of our results may need to be reassessed and more mature modeling developed. However, this approach seems likely to exhibit features that will survive, at least in part, in a more mature description.

There is an obvious question as to the reliability of our nonrelativistic treatment for light flavors. We suggest, however, that the physics of the excitation is probably more general than the specific modeling herein. For very massive quarks, where the nonrelativistic treatment may be justified, the c.m. of the system tends to lie on the interquark axis $\vec{r} \equiv \vec{r}_Q - \vec{r}_{\bar{Q}}$. For $|\vec{q}| < m_Q$ the recoil of the quark is small and the c.m. tends to remain near this axis. As a consequence, we find that excitation of the tube is suppressed. As the quark masses are reduced, the c.m. of the system can have increasingly large excursions from the $\vec{r}$ axis, and the tube is more easily excited. There comes a point where the quarks are light and the nonrelativistic approximations are suspect; however, the physical picture that the flux-tube excitation is easier for this situation than for the heavy quark case is a physically reasonable extrapolation. So although the actual numbers may be debatable, the probability for excitation of the flux tube seems likely to be at least as big as was calculated for massive quarks where the nonrelativistic approximations still apply. The J^{PC} patterns of the results and the conclusions about charge exchange processes being required for the excitation of hybrids in the $E1$ multipole also seem to be robust.

Our results suggest a way of assessing the flux-tube excitation in a lattice QCD approach. For an $E1$ transition with no spin flip, a π can be excited to axial mesons. The electrically charged hybrid ($a^{\pm}_{1H}$) and conventional ($b^{\pm}_1$) axial states thus excited have opposite G parities. Thus the relative strength of the matrix elements for electromagnetic $E1$ transition to G parity ± 1 gives a measure of the penalty for exciting the flux tube.

It will be interesting to see if lattice QCD simultaneously can describe the magnitude of $\langle r^2 \rangle_\pi$, the $E1$ amplitudes for exciting $G = \pm 1$ axial mesons, and test the extent to which the electric dipole sum rule relating these is saturated. In our approximations we see that it is saturated by the $^1P_1$ conventional states and their hybrid axial counterparts. If these results are verified, then it may be possible to extrapolate to other multipoles, relating the modifications of various static properties by the flux-tube degrees of freedom to the excitation of hybrid states of various J^{PG}.

The hybrid configurations with nonexotic J^{PC} will tend to mix into the wave functions of the conventional mesons. Unless specific observables (such as g_A/g_V) have anomalous values, it will be hard to make a convincing case for such states. If the enhancement in $B \to \psi X$ can be shown to be due to a K_A state, this would be very interesting but would not of itself be proof of a hybrid. Further measurements of polarization or g_A/g_V would be needed to distinguish it from a radial excitation of a conventional axial. The main interest is seeking rates for states with exotic J^{PC}. Table II and Eq. (25) predict healthy couplings to $\gamma\rho$, which implies that photoexcitation of 0^{+-},2^{+-} off a ρ is feasible in charge exchange. We note also that diffractive production of 2^{+-} with photon beams is to be expected; hence, 2^{+-} exotic states should be searched for in charge exchange and also in diffractive scattering—e.g., at either Jefferson Lab or HERA. This is discussed further in [25].

In the decays of heavy flavors $B \to D_H X$ hides the exotic quantum numbers in the flavor of the D_H. However, the ''spin inversion'' between conventional and hybrid vector mesons (the hybrid being a quark spin singlet in contrast to the conventional triplet) leads to an interesting selection rule $B^0 \to \pi^- D^+_H(1^{-(-)}) \equiv 0$. Hence observation of a vector D^* in other processes, which is absent in B decay, could be a signature for $D_H(1^-)$.

The production of an axial strange hybrid in $B \to \psi K_H$ is predicted to have BR$\sim O(10^{-4})$ as long as its mass $\leqslant 2.1$ GeV. There is a tantalizing unexplained enhancement in the data that may be compatible with this and merits further investigation. This process superficially has an analogue in $B \to D^{*0} n\bar{n}_H$, which opens up the available phase space for $n\bar{n}$ to ~ 3 GeV, enabling light-flavored hybrid states with exotic quantum numbers to be produced. Unlike the previous case, however, there is the possibility that rescattering effects and the failure of factorization could contaminate our analysis of this process. Modulo this caveat, we have BR$(B \to D^{*0}(n\bar{n})_H) \sim O(10^{-5})$ for $\pi_1(1600)$; if this is the exotic hybrid with $J^{PC} = 1^{-+}$; $(0,2)^{+-}$, exotics have potentially even larger rates provided they have masses below 3 GeV.

The exotic 1^{-+} resonance $\pi_1(1600)$ could in principle be looked for in D decays. We find a branching ratio for $D \to \pi\pi_1(1600)$ that is $\sim 10^{-4}$ times that for $D \to \pi\rho$. Folding in the predicted [25,35] BR$(\pi_1(1600) \to \pi\rho) \sim 20\%$ gives a combined branching ratio to $\pi\pi\rho$ via this exotic of $\sim 10^{-8}$. This would be a severe challenge even for high statistics studies that may become available at CLEO-c or GSI.

This exotic should have $I = 0$ partners if it is indeed a hybrid and not some dimeson effect. The $s\bar{s}_H$ state can be produced in leading order $D_s \to \pi s\bar{s}_H$ if its mass is below 1.9

GeV. If the nonet is not ideal, then there is the hope of some $s\bar{s}$ content in each of the $I=0$ states, one hopefully light enough to be accessible. Similar to the above, we find a branching ratio that is $\sim 10^{-4}$ times that for $D_s \to \pi\phi$. Here, again, one is at best at the limits of detection. Another potential source of these exotic hybrids is in the decay $B_s \to J/\psi s\bar{s}_H$ which is the s-quark spectator analogue of $B \to J/\psi K_H$. We find a branching fraction for a 1^{-+} $s\bar{s}$ hybrid at 1.9 GeV to be $\sim 6\times 10^{-6}$ which is far lower than current statistics can observe.

The general formalism developed here can be applied to any current induced transition. Examples include gluon emissions (as in $c\bar{c}$ cascades), diffractive excitation, or π emission where the pion is treated as an effective γ_5 current. The latter has a long and successful history in describing conventional hadron decays [36,37] and can now be applied analogously to the production or decays of hybrids involving π. This is described in Ref. [25].

ACKNOWLEDGMENTS

This work is supported, in part, by grants from the Particle Physics and Astronomy Research Council, and the EU-TMR program ''Euridice,'' HPRN-CT-2002-00311. We thank P.J.S. Watson and J. Paton for discussions on the dynamics of flux tubes.

APPENDIX A: HYBRID TRANSITION OPERATOR FOR V_μ AND A_μ

We perform the nonrelativistic reduction of the vector and axial currents allowing for flavor changing. We present the particular case of $B(b\bar{d}) \to D(c\bar{d})$ by quark level $b \to c$. In the following $m_D = m_d + m_c$ and $m_B = m_d + m_b$, which are indeed the meson masses in the extreme nonrelativistic limit.

V^0: For the zeroth (time) component of the vector current we have

$$V^0(p_c,p_b;x) = \bar{c}(x)\gamma^0 b(x) \xrightarrow{\text{N.R.}} e^{i(p_c-p_b)\cdot x} \times\left\{1+\frac{\vec{p}_c\cdot\vec{p}_b}{4m_b m_c}+\frac{i}{4}\vec{\sigma}\cdot\left(\frac{\vec{p}_c}{m_c}\wedge\frac{\vec{p}_b}{m_b}\right)+\cdots\right\}. \tag{A1}$$

Considering only the terms linear in $\vec{a}$ obtained from utilizing the effect of the momentum operator on flux-tube ground state wave functions,

$$\vec{p}\,|\chi_0\rangle|_{\vec{a}\text{-cmpt}} = -i\sqrt{\frac{2b}{\pi}}\beta_1\vec{a}\,|\chi_0\rangle, \tag{A2}$$

and expanding the plane wave to leading order in $\vec{q}\cdot\vec{a}$ we have the effective transition operator to the first hybrid excitation:

$$V_H^0 = e^{-i\vec{q}\cdot\vec{r}(m_d/m_D)}\sqrt{\frac{2b}{\pi^3}}\beta_1 \times\left\{i\vec{q}\cdot\vec{a}\left(\frac{2r}{m_D}+\frac{\pi}{4m_b m_c}\right)-\frac{\pi}{4m_b m_c}\vec{\sigma}\cdot\vec{q}\wedge\vec{a}\right\}. \tag{A3}$$

$\vec{V}$: For the spatial vector current we have

$$\vec{V}(p_c,p_b;x) = \bar{c}(x)\vec{\gamma}b(x) \xrightarrow{\text{N.R.}} e^{i(p_c-p_b)\cdot x} \times\left\{\left(\frac{\vec{p}_b}{2m_b}+\frac{\vec{p}_c}{2m_c}\right) - i\vec{\sigma}\wedge\left(\frac{\vec{p}_b}{2m_b}-\frac{\vec{p}_c}{2m_c}\right)+\cdots\right\} \tag{A4}$$

and the relevant transition to first excited hybrid becomes

$$\vec{V}_H = e^{-i\vec{q}\cdot\vec{r}(m_d/m_D)}\sqrt{\frac{2b}{\pi^3}}\beta_1\left\{-i\frac{\pi}{2m_b}\left(\frac{m_b}{m_c}+1\right)\vec{a} - i\frac{r}{m_c m_D}(\vec{q}\cdot\vec{a})\vec{q}+\frac{\pi}{2m_b}\left(\frac{m_b}{m_c}-1\right)\vec{\sigma}\wedge\vec{a} + \frac{r}{m_c m_D}(\vec{q}\cdot\vec{a})\vec{\sigma}\wedge\vec{q}\right\}. \tag{A5}$$

A^0:

$$A^0(p_c,p_b;x) = \bar{c}(x)\gamma^0\gamma^5 b(x) \xrightarrow{\text{N.R.}} e^{i(p_c-p_b)\cdot x} \times\left\{\vec{\sigma}\cdot\left(\frac{\vec{p}_b}{2m_b}+\frac{\vec{p}_c}{2m_c}\right)+\cdots\right\} \tag{A6}$$

and the relevant hybrid transition becomes

$$A_H^0 = e^{-i\vec{q}\cdot\vec{r}(m_d/m_D)}\sqrt{\frac{2b}{\pi^3}}\beta_1 \times\left\{-i\frac{\pi}{2m_b}\left(\frac{m_b}{m_c}+1\right)\vec{\sigma}\cdot\vec{a}-i\frac{r}{m_c m_D}(\vec{q}\cdot\vec{a})\vec{\sigma}\cdot\vec{a}\right\}. \tag{A7}$$

$\vec{A}$:

$$\vec{A}(p_c,p_b;x) = \bar{c}(x)\vec{\gamma}\gamma^5 b(x) \xrightarrow{\text{N.R.}} e^{i(p_c-p_b)\cdot x} \times\left\{\vec{\sigma}\left(1-\frac{\vec{p}_c\cdot\vec{p}_b}{4m_c m_b}\right) + \frac{\vec{p}_b(\vec{\sigma}\cdot\vec{p}_c)+\vec{p}_c(\vec{\sigma}\cdot\vec{p}_b)}{4m_c m_b}-i\frac{\vec{p}_c\wedge\vec{p}_b}{4m_c m_b}\right\} \tag{A8}$$

and the relevant hybrid transition becomes

TABLE V. $\mathcal{D}^{(1)}_{m'm}(\phi,\theta,-\phi)$.

$m'\backslash m$	$+1$	0	-1
$+1$	$\frac{1}{2}(1+\cos\theta)$	$-\frac{1}{\sqrt{2}}e^{-i\phi}\sin\theta$	$\frac{1}{2}e^{-2i\phi}(1-\cos\theta)$
0	$\frac{1}{\sqrt{2}}e^{i\phi}\sin\theta$	$\cos\theta$	$-\frac{1}{\sqrt{2}}e^{-i\phi}\sin\theta$
-1	$\frac{1}{2}e^{2i\phi}(1-\cos\theta)$	$\frac{1}{\sqrt{2}}e^{i\phi}\sin\theta$	$\frac{1}{2}(1+\cos\theta)$

$$\vec{A}_H = e^{-i\vec{q}\cdot\vec{r}(m_d/m_D)}\sqrt{\frac{2b}{\pi^3}}\beta_1\left\{ i(\vec{q}\cdot\vec{a})\vec{\sigma}\left(\frac{2r}{m_D}-\frac{\pi}{4m_bm_c}\right) + i\frac{\pi}{4m_bm_c}[(\vec{\sigma}\cdot\vec{a})\vec{q}+(\vec{\sigma}\cdot\vec{q})\vec{a}]+\frac{\pi}{4m_bm_c}\vec{q}\wedge\vec{a}\right\}. \tag{A9}$$

APPENDIX B: HOW TO CALCULATE THE TRANSITION TO A HYBRID

We consider the generic

$$\mathcal{M}\equiv\langle \mathrm{hyb};\pm,m'|\mathcal{O}_{\mathrm{ref}}|\mathrm{conv};l,m\rangle = \int d^3\vec{r}\int d^2\vec{a}\,\mathcal{H}^*\mathcal{O}_{\mathrm{ref}}\mathcal{C},$$

where $\mathcal{O}_{\mathrm{ref}}\equiv\vec{a}\cdot\vec{x}_i$ and the $\pm$ is the hybrid state flux-tube polarization. In this specific example we shall choose $\vec{x}_-\equiv\hat{x}-i\hat{y}$ and calculate the matrix element

$$\langle\chi_1,\pm|\vec{a}\cdot\vec{x}_-|\chi_0\rangle \equiv -\langle\chi_1,\pm|(a_1+ia_2)\mathcal{D}^{(1)*}_{-+} -(a_1-ia_2)\mathcal{D}^{(1)*}_{--}|\chi_0\rangle,$$

where we have introduced the $\mathcal{D}$ rotation functions shown explicitly for $j=1$ in Table V.

The explicit expression for the matrix element is

$$-\int d^2\vec{a}\,\beta_1(a_1\mp ia_2)[(a_1+ia_2)\mathcal{D}^{(1)*}_{-+} -(a_1-ia_2)\mathcal{D}^{(1)*}_{--}]|\chi_0(a_1)|^2|\chi_0(a_2)|^2,$$

where the χ_0 are as in Eq. (5).

Rewrite $a_1\pm ia_2\equiv a^{\pm}$ and the integral becomes

$$-\beta_1\int d^2\vec{a}\,a^{\mp}(a^+\mathcal{D}^{(1)*}_{-+}-a^-\mathcal{D}^{(1)*}_{--})|\chi_0(a_1)|^2|\chi_0(a_2)|^2.$$

Now use $a^+a^-=a_1^2+a_2^2$ and note that $a^{\pm}a^{\pm}$ vanishes under integration. This brings us to

$$-\beta_1\int d^2\vec{a}(a_1^2+a_2^2)(\delta^+\mathcal{D}^{(1)*}_{-+}-\delta^-\mathcal{D}^{(1)*}_{--}) \times|\chi_0(a_1)|^2|\chi_0(a_2)|^2.$$

Then using the integral

$$\int d^2\vec{a}(a_1^2+a_2^2)|\chi_0(a_1)|^2|\chi_0(a_2)|^2 = \frac{\beta_1^2}{\pi}\int d^2\vec{a}(a_1^2+a_2^2)e^{-\beta_1^2(a_1^2+a_2^2)}=\beta_1^{-2},$$

we finally obtain the essential angular decompositions as follows:

$$\langle\chi_1,\pm|\vec{a}\cdot\vec{x}_-|\chi_0\rangle = -\frac{1}{\beta_1}(\delta^+\mathcal{D}^{(1)*}_{-+}-\delta^-\mathcal{D}^{(1)*}_{--}), \tag{B1}$$

$$\langle\chi_1,\pm|\vec{a}\cdot\vec{x}_+|\chi_0\rangle = +\frac{1}{\beta_1}(\delta^+\mathcal{D}^{(1)*}_{++}-\delta^-\mathcal{D}^{(1)*}_{+-}), \tag{B2}$$

$$\langle\chi_1,\pm|\vec{a}\cdot\hat{z}|\chi_0\rangle = -\frac{1}{\sqrt{2}\beta_1}(\delta^+\mathcal{D}^{(1)*}_{0+}-\delta^-\mathcal{D}^{(1)*}_{0-}). \tag{B3}$$

To proceed from Eq. (18) first expand the exponential in terms of partial wave angular states $\equiv\Sigma_L i^L(2L+1)\mathcal{D}^{(L)*}_{00}j_L(-|\vec{q}|r(\mu/m_Q))$, contract together the three $\mathcal{D}$ functions,

$$\left[\int d\Omega\mathcal{D}^{(1)}_{m',\pm}\mathcal{D}^{(L)*}_{00}(\delta^+\mathcal{D}^{(1)*}_{-+}-\delta^-\mathcal{D}^{(1)*}_{--})\right]^* = \frac{4\pi}{3}\langle L0;1-1|1m'\rangle(\delta^+\langle L0;1+1|1+1\rangle -\delta^-\langle L0;1-1|1-1\rangle),$$

and integrate $\int d\Omega$, which gives, for the matrix element,

$$-\frac{1}{\beta_1}\frac{1}{\sqrt{3}}\sum_L i^L(2L+1)\,{}_f\langle j_L\rangle_i\langle L0;1-1|1m'\rangle \times(\delta^+\langle L0;1+1|1+1\rangle-\delta^-\langle L0;1-1|1-1\rangle)$$

and, finally,

$$-\frac{1}{\beta_1}\frac{1}{\sqrt{3}}\delta_{m',-1}\left[\left({}_f\langle j_0\rangle_i-\frac{1}{2}{}_f\langle j_2\rangle_i\right)(\delta^+-\delta^-) -i\frac{3}{2}{}_f\langle j_1\rangle_i(\delta^++\delta^-)\right],$$

where we now only need to calculate the radial expectation values of the spherical Bessel functions.

TABLE VI. β values and state masses in GeV.

	$L=0$ $\frac{2}{\pi^{1/4}}\beta_{1S}^{3/2}e^{-\beta_{1S}^2 r^2/2}$		$L=1$ $\frac{2}{\pi^{1/4}}\sqrt{\frac{2}{3}\beta_{1P}^{5/2}\, r\, e^{-\beta_{1P}^2 r^2/2}}$		Hybrid $\sqrt{\frac{2}{\Gamma(3/2+\delta)}}\beta_H^{\frac{3}{2}+\delta} r^{\delta} e^{-\beta_H^2 r^2/2}$	
	β_{1S}	M_{1S}	β_{1P}	M_{1P}	β_H	M_H
$n\bar{n}$	0.334	0.672	0.280	1.296	0.260	1.825
$n\bar{s}$	0.370	0.780	0.306	1.386	0.275	1.961
$s\bar{s}$	0.426	0.857	0.342	1.448	0.311	2.024
$n\bar{c}$	0.389	2.036	0.331	2.544	0.291	3.128
$s\bar{c}$	0.469	2.092	0.387	2.571	0.335	3.195
$c\bar{c}$	0.639	3.129	0.509	3.539	0.426	4.235
$n\bar{b}$	0.408	5.392	-	-	0.302	6.449
$s\bar{b}$	0.510	5.455	-	-	0.355	6.563
$c\bar{b}$	0.798	6.418	-	-	0.486	7.575
$b\bar{b}$	1.239	9.522	-	-	-	-

APPENDIX C: "DIPOLE" FORM IN THE ADIABATIC FLUX-TUBE MODEL

In the usual nonrelativistic quark model the matrix element of the lowest order electric dipole operator $\sim\vec{\epsilon}\cdot\vec{p}/m$ can be transformed using the commutator $\vec{p}=im[H,\vec{r}]$ into an explicit dipole form $\sim|\vec{q}|\vec{\epsilon}\cdot\vec{r}$. This commutation relation is valid provided the system Hamiltonian can be written in the form $H=p^2/2m+V(r)$, any other dependence of $\vec{p}$ causing deviations from this behavior. We find that this transformation is justified in the adiabatic approximation to the flux-tube model also.

Minimal coupling of the photon field to a quark at $\vec{r}_Q$ moving with $\vec{p}_Q$ leads to a convection current operator $\sim\vec{p}_Q\cdot\vec{A}(\vec{r}_Q)$. For a plane-wave photon field at lowest order in $\vec{q}\cdot\vec{r}_Q$ we get an E1 operator $\sim\vec{\epsilon}\cdot\vec{p}_Q/m_Q$.

We construct $\vec{p}_Q$ as follows:

$$\vec{p}_Q\equiv m\dot{\vec{r}}_Q=-\frac{m_Q(m_d+br/2)}{m_Q+m_d+br}\dot{\vec{r}} -\frac{b}{\pi}\sqrt{\frac{2}{N+1}}\frac{d}{dt}\left(r\sum_p \vec{a}_p/p\right). \quad \text{(C1)}$$

The second term is linear in $\vec{a}$ and can hence excite the flux-tube. Using the identity $(d/dT)A=i[H,A]$ we can write the flux tube term as

$$-\frac{b}{\pi}\sqrt{\frac{2}{N+1}}\, i\left[H,r\sum_p \vec{a}_p/p\right]. \quad \text{(C2)}$$

Then

$$\langle\mathcal{H}|\vec{p}_Q|\mathcal{C}\rangle=-\frac{ib}{\pi}\sqrt{\frac{2}{N+1}}(E_{\mathcal{H}}-E_{\mathcal{C}})\langle\mathcal{H}|r\sum_p \vec{a}_p/p|\mathcal{C}\rangle =-\frac{ib}{\pi}\sqrt{\frac{2}{N+1}}|\vec{q}|\langle\mathcal{H}|r\sum_p \vec{a}_p/p|\mathcal{C}\rangle, \quad \text{(C3)}$$

and hence

$$\langle\mathcal{H}|\frac{\vec{\epsilon}\cdot\vec{p}_Q}{m_Q}|\mathcal{C}\rangle=i|\vec{q}|\langle\mathcal{H}|\vec{\epsilon}\cdot\vec{r}_Q|\mathcal{C}\rangle, \quad \text{(C4)}$$

so that using the dipole form is justified in the flux-tube case.

APPENDIX D: HYBRID HAMILTONIAN

We follow the formulation of the flux-tube model described in [3,38,39]. In the appendix of [3] the authors show explicitly that the spatial wave function of a hybrid state with phonon occupation $\{n_{p+},n_{p-}\}$ can be written

$$R_{nLN\Lambda}(r)\sqrt{\frac{2L+1}{4\pi}}\mathcal{D}^{(L)*}_{m_L\Lambda}(\phi,\theta,-\phi),$$

where the quantum numbers are n, radial; (L,m_L), angular momentum; $N=\Sigma_p(n_{p+}+n_{p-})$; $\Lambda=\Sigma_p(n_{p+}-n_{p-})$. We are only interested in the lightest hybrids which have one phonon excited in the $p=1$ mode and hence $N=1$ and $\Lambda=\pm1$. In the adiabatic approximation we get a radial Hamiltonian [acting on $rR(r)$] for these hybrids,

$$H^1=\frac{1}{2\mu}\frac{\partial^2}{\partial r^2}+\frac{L(L+1)-\Lambda^2}{2\mu r^2}+br +\frac{\pi}{r}(1-e^{-f\sqrt{b}r})-\frac{\kappa}{r}+c, \quad \text{(D1)}$$

whereas for conventional mesons (no phonons) we would get

$$H^0=\frac{1}{2\mu}\frac{\partial^2}{\partial r^2}+\frac{L(L+1)}{2\mu r^2}+br-\frac{\kappa}{r}+c.$$

The modified angular momentum barrier in the hybrid case has its origin in the $\Lambda=\pm1$ carried by the phonon in the tube. br is the mass energy of the string. π/r is the excitation

energy of the string in the $p=1$ mode; the additional factor multiplying this is put in by hand and is designed to model the fact that at short distances we do not expect "stringy" configurations to dominate in QCD. The remaining potential terms $-\kappa/r+c$ are introduced by hand, the first of which represents one-gluon-exchange dominance at short distances and the second is required to describe the observed meson spectrum.

The parameters m_Q, b, κ, c are chosen to reproduce approximately the observed conventional meson spectrum (up to spin-dependent splittings). We use the set of values $b=0.18$ GeV^2, $f=1$, $c=-0.7$ GeV, $m_{u,d}=0.33$ GeV, $m_s=0.55$ GeV, $m_c=1.77$ GeV, $m_b=5.17$ GeV. κ is allowed to run in a reasonable way so that for light mesons $(n\bar{n}, n\bar{s}, s\bar{s})$ $\kappa=1.07$, for heavy-light mesons $(n\bar{c}, s\bar{c}, n\bar{b}, s\bar{b})$ $\kappa=0.67$, and for heavy-heavy mesons $(c\bar{c}, c\bar{b}, b\bar{b})$ $\kappa=0.52$.

We solve the Schrödinger equation variationally using a harmonic-oscillator basis

$$R^{HO}_{n,L'}(r)=\sqrt{\frac{2\Gamma(n)}{\Gamma(n+L'+1/2)}}\beta^{L'+3/2}r^{L'}\times\mathcal{L}^{L'+1/2}_{n-1}(\beta^2r^2)e^{-\beta^2r^2/2}.$$

For conventional states L' here is just the angular momentum quantum number L. For the hybrid Hamiltonian the modified angular momentum barrier is canceled if L' is chosen so it satisfies $L'(L'+1)=L(L+1)-\Lambda^2$; for $L=1,\Lambda=\pm1$, this means $L'\equiv\delta\approx0.62$.

The Hamiltonians H^0, H^1 are found to be diagonal in this basis to a very good approximation if the β values listed in Table VI are used.

Merlin [39] and Merlin and Paton [38] consider nonadiabatic corrections to this Hamiltonian; the values quoted in Table VI are actually obtained using this modified Hamiltonian, although the differences in β with respect to using H^1 are usually small.

[1] SESAM Collaboration, G. Bali *et al.*, Nucl. Phys. B (Proc. Suppl.) **63**, 209 (1997); IBM Collaboration, J. Sexton *et al.*, Phys. Rev. Lett. **75**, 4563 (1995); F.E. Close and M.J. Teper, Report No. RAL-96-040/OUTP-96-35P; C.J. Morningstar and M. Peardon, Phys. Rev. D **56**, 4043 (1997); D. Weingarten, Nucl. Phys. B (Proc. Suppl.) **53**, 232 (1997); **63**, 194 (1998); **73**, 249 (1999); C. McNeile and C. Michael, Phys. Rev. D **63**, 114503 (2001).

[2] P. Lacock, C. Michael, P. Boyle, and P. Rowland, Phys. Lett. B **401**, 308 (1997); C. Bernard *et al.*, Phys. Rev. D **56**, 7039 (1997); P. Lacock and K. Schilling, Nucl. Phys. B (Proc. Suppl.) **73**, 261 (1999); C. McNeile, hep-lat/9904013; C. Morningstar, Nucl. Phys. B (Proc. Suppl.) **90**, 214 (2000).

[3] N. Isgur and J. Paton, Phys. Rev. D **31**, 2910 (1985).

[4] N. Isgur, R. Kokoski, and J. Paton, Phys. Rev. Lett. **54**, 869 (1985).

[5] F.E. Close and P.R. Page, Nucl. Phys. **B443**, 233 (1995).

[6] C. Michael, hep-ph/0009115.

[7] *Quark Confinement and the Hadron Spectrum II*, edited by N. Brambilla and G.M. Prosperi (World Scientific, Singapore, 1997).

[8] K.J. Juge, J. Kuti, and C. Morningstar, Phys. Rev. Lett. **90**, 161601 (2003).

[9] B. Lasscock, D.B. Leinweber, A.W. Thomas, and A.G. Williams (unpublished) and (private communication).

[10] C. Michael, Phys. Rev. D **65**, 094505 (2002).

[11] F.E. Close and P.R. Page, Phys. Rev. D **52**, 1706 (1995).

[12] A. Afanasev and P.R. Page, Phys. Rev. D **57**, 6771 (1998).

[13] BABAR Collaboration, B. Aubert *et al.*, Phys. Rev. D **67**, 032002 (2003).

[14] E852 Collaboration, G. Adams *et al.*, Phys. Rev. Lett. **81**, 5760 (1998).

[15] VES Collaboration, Y. Khokhlov *et al.*, Nucl. Phys. **A663**, 596 (2000).

[16] VES Collaboration, V. Dorofeev, hep-ex/9905002.

[17] E852 Collaboration, I.I. Ivanov *et al.*, Phys. Rev. Lett. **86**, 3977 (2001).

[18] N. Isgur, Phys. Rev. D **60**, 114016 (1999).

[19] T. Barnes, F.E. Close, and E.S. Swanson, Phys. Rev. D **52**, 5242 (1995).

[20] F.E. Close and J. Dudek, in Proceedings of HUGS School, Jefferson Laboratory, 2003.

[21] Particle Data Group, D. Groom *et al.*, Eur. Phys. J. C **15**, 1 (2000).

[22] F.E. Close and J.J. Dudek, Phys. Rev. Lett. **91**, 142001 (2003).

[23] F.E. Close, A. Donnachie, and Yu.S. Kalashnikova, Phys. Rev. D **65**, 092003 (2002).

[24] E.S. Swanson, Ann. Phys. (N.Y.) **220**, 73 (1992).

[25] F.E. Close and J. Dudek, "The forbidden decays of hybrids to $\pi\rho$ can be large," hep-ph/0308099.

[26] "The Science Driving the 12 GeV Upgrade of CEBAF" (Jefferson Lab, 2001), edited by L. Cardman *et al.* (unpublished).

[27] M. Neubert and B. Stech, Adv. Ser. Direct. High Energy Phys. **15**, 294 (1998).

[28] N. Isgur, D. Scora, B. Grinstein, and M. Wise, Phys. Rev. D **39**, 799 (1989).

[29] C.K. Chua, W.S. Hou, and G.G. Wong, Phys. Rev. D **68**, 054012 (2003).

[30] G. Chiladze, A.F. Falk, and A.A. Petrov, Phys. Rev. D **58**, 034013 (1998).

[31] J. Dudek, "The structure of B and D hybrid states in the flux tube model" (in preparation).

[32] S. Mantry, D. Pirjol, and I.W. Stewart, Phys. Rev. D **68**, 114009 (2003).

[33] D. Scora and N. Isgur, Phys. Rev. D **52**, 2783 (1995).

[34] CLEO Collaboration, K.W. Edwards *et al.*, Phys. Rev. D **65**, 012002 (2002).

[35] P.R. Page, Phys. Lett. B **415**, 205 (1997).

[36] R.P. Feynman, M. Kislinger, and F. Ravndal, Phys. Rev. D **3**, 2706 (1971).

[37] S. Godfrey and N. Isgur, Phys. Rev. D **32**, 189 (1985).

[38] J. Merlin and J. Paton, J. Phys. G **11**, 439 (1985).

[39] J. Merlin, Ph.D. thesis, University of Oxford, 1986.